Serpentinised peridotites from an ultrahigh-pressure terrane in the Pohorje Mts. (Eastern Alps, Slovenia): Geochemical constraints on petrogenesis and tectonic setting

Cite As: De Hoog, C-J, Janák, M, Vrabec, M & Froitzheim, N 2009, 'Serpentinised peridotites from an ultrahigh-pressure terrane in the Pohorje Mts. (Eastern Alps, Slovenia): Geochemical constraints on petrogenesis and tectonic setting' *Lithos*, vol 109, no. 3-4, pp. 209-222.

Serpentinised peridotites from an ultra-high pressure terrane in the Pohorje Mts. (Eastern Alps, Slovenia): Geochemical constraints on petrogenesis and tectonic setting

Jan C. M. De Hoog [a, b] ✉

Marian Janák [c]

Mirijam Vrabec [d]

Nikolaus Froitzheim [e]

[a] Earth Science Centre, Göteborg University, 405 30 Göteborg, Sweden

[b] Present address: Dept of Earth Sciences, University of Oxford, Parks Road, OX1 3PR, Oxford, Great Britain

[c] Geological Institute, Slovak Academy of Sciences, Dúbravská 9, PO Box 106, 840 05 Bratislava 45, Slovak Republic

[d] Department of Geology, University of Ljubljana, Aškerčeva 12, 1000 Ljubljana, Slovenia

[e] Steinmann-Institut, Universität Bonn, Nussallee 8, D-53115 Bonn, Germany

Revised manuscript submitted for publication in:

Lithos

Special Volume dedicated to Tony Carswell

✉ Corresponding author
Email : cees-jan@earth.ox.ac.uk
Tel.: +44 1865 282113
Fax: +44 1865 272072

Abstract

The Slovenska Bistrica ultramafic complex (SBUC; Eastern Alps, Slovenia) occupies the south-eastern most part of the Pohorje Mountains, which represent an exhumed piece of continental crust subducted during the Cretaceous Eo-Alpine orogeny. The SBUC is composed of serpentinised harzburgites with local occurrences of garnet lherzolite, and is the only known occurrence of ultramafic rocks within the high- to ultrahigh-pressure nappe system apart from a few small dismembered pieces in the near vicinity. The harzburgites are highly depleted following melting within the spinel stability field, as exemplified by high whole-rock MgO contents (41.5-44.3 wt%), low Al_2O_3 (0.7-1.2 wt%), low Lu_N (0.1-0.7), and high Cr# of Cr-spinel (0.4-0.9). Fluid-immobile incompatible trace elements (Ti, Sc, V, Zr, HREE, Th) correlate well with MgO, consistent with a melt depletion trend. Other incompatible elements (Ba, Sr, LREE) show little correlation and are probably modified by the serpentinisation process or later metamorphic overprint. However, comparable LREE enrichment of all samples and absence of negative Nb and Th anomalies suggests that this piece of mantle was already metasomatised by melts or fluids before serpentinisation. Garnet lherzolite in the SBUC recorded an UHP stage (4 GPa, 900°C) not visible in the harzburgites. Because of the evidence of an earlier lower pressure stage within the spinel stability field, the SBUC represents a piece of subducted mantle. The protolith of the harzburgites is probably oceanic mantle, considering the high degree of melt depletion yet the lack of a subduction-zone signature. It therefore most likely represents a part of previously subducted Meliata oceanic mantle, which was part of a deeper section of the hanging wall along which subduction of the continental crust that is now exposed in Pohorje took place. Alternatively, it may represent mantle depleted and metasomatised in a continental rift zone, which was later incorporated in the hanging wall of the subduction zone and subsequently dragged down to UHP conditions.

Keywords: Pohorje, serpentinite, harzburgite, mantle melting, metasomatism, continental subduction

1. Introduction

Ultramafic rocks are a small but common component of continental crust that has gone through a subduction and exhumation cycle (e.g., Scandinavian Caledonides, Medaris and Carswell, 1990, Ravna et al., 2006; Dabie-Sulu terrane, Liou and Zhang, 1998, Yang and Jahn, 2000; Bohemian Massif, Medaris et al., 1990). Petrologically the rocks vary widely from pyroxenites to lherzolites to harzburgites, include garnet and spinel-bearing varieties and occur as boudins and lenses or as larger orogenic bodies within the continental crust.

Most of these ultramafic rocks are interpreted to be derived from the overlying mantle wedge, and may have been incorporated at great depth and high pressure, but also at lower pressure and subsequently subducted together with the down-going continental plate (Medaris, 2000; Brueckner and Medaris, 2000). Alternatively, the ultramafics may have been present in the continental crust before subduction.

The significance of these ultramafic rocks is manifold. If garnet-bearing they can provide independent proof of an high to ultrahigh-pressure stage of the rocks (e.g., Carswell, 1986; Janák et al., 2006). Their former tectonic setting and melt depletion ages may provide important clues as to the tectonic history of the region before the subduction stage (e.g., Spengler et al., 2006; Yuan et al., 2007) and put constraints on the subduction process itself. They also may provide information about metasomatic processes before and during subduction, and, if serpentinised, may facilitate exhumation of subducted rocks (Guillot et al., 2000).

The Pohorje Mountains in Slovenia, part of the Eastern Alps, have recently been established as a terrane with peak metamorphic conditions within the coesite stability field, i.e., ultrahigh-pressure (UHP) conditions (Janák et al., 2004), and associated with eclogite UHP localities several outcrops of garnet peridotites have been found (Janák et al., 2006; Vrabec, 2007). The

largest ultramafic body is strongly serpentinised, comprising the south eastern-most extension of the Pohorje Mountains (Hinterlechner-Ravnik et al., 1991a), and has previously been suggested to be a former layered gabbro (Visona et al., 1991). Janák et al. (2006) investigated UHP garnet peridotites from within and nearby the ultramafic body and proposed that these could have been derived from depleted mantle rocks that were subsequently metasomatised by melts and/or fluids either in the plagioclase-peridotite or the spinel-peridotite field.
In this paper we focus on the serpentinised ultramafic body and aim to reconstruct its geological and tectonic history. Albeit strongly serpentinised, the body retained a signature of extensive melt depletion, either in a continental rift or an oceanic ridge environment. It therefore probably represents a sliver of overlying mantle tectonically emplaced in the continental crust during subduction. UHP metamorphism was recorded locally in garnet peridotites.

1.1. Geological background

Ultramafic rocks occur in the south-easternmost part of the Pohorje Mountains. Near Slovenska Bistrica (Fig. 1) they form a body of ca. 6×1.5 km size, which is termed the "Slovenska Bistrica ultramafic complex" (SBUC; Janák et al., 2006). The main protoliths of the SBUC were described as harzburgites and dunites by Hinterlechner-Ravnik et al. (1991a). Because of extensive serpentinisation, only a few less altered garnet peridotites, garnet pyroxenites and coronitic metatroctolites are preserved (Hinterlechner-Ravnik et al., 1991a; Janák et al., 2006). The ultramafics include numerous lenses, boudins and bands of eclogites. The country rocks enclosing the SBUC consist of a typical continental crust assemblage of high-grade metamorphic rocks, such as ortho- and paragneisses, micaschists, amphibolites

and marbles (Mioč and Žnidarčič, 1977; Hinterlechner-Ravnik et al., 1991a, b; Janák et al., 2004; Miller et al., 2005). These rocks form a strongly foliated matrix around elongated lenses and boudins of eclogite and ultramafics, including the SBUC. Abundant eclogites record peak pressures from 2.4 to 3.2 GPa (Sassi et al., 2004; Janák et al., 2004; Vrabec, 2004, 2007), with the highest values in the southeast near the SBUC (Janák et al., 2004), whereas garnet-bearing peridotites and pyroxenites record peak pressures of up to 4 GPa (Janák et al., 2006).

1.2. Tectonic history

The region has a complicated tectonic history, which was reconstructed by Schmid et al. (2004 and references therein). A short summary is given here. The current Austroalpine nappes of the Eastern Alps were part of a continental block called Apulia that was bordered to the east by the Meliata ocean, an extension of the Neotethys ocean. The Meliata ocean opened in the Middle Triassic, and oceanic crust was produced there during the Late Middle and Upper Triassic. The Meliata ocean was subducted towards southeast during the Jurassic, until in the Late Jurassic the Apulian continental margin collided with the volcanic arc of the subduction zone. At the same time (Middle Jurassic) rifting more northwards in response to the opening of the Atlantic ocean resulted in opening of the Piedmont-Liguria ocean. Continued convergence within Apulia during the Cretaceous was accommodated north-westwards of the Meliata suture by intra-continental subduction, probably along the location of a failed Permian rift, resulting in thrusting and nappe stacking onto the northern part of the Apulian continental block (Janák et al., 2004). The subducted crust underwent high-P metamorphism, which is still preserved in Eo-Alpine eclogites. Slab extraction resulted in partial exhumation of the subducted crust (Janák et al., 2004, 2006).

The timing of HP and UHP metamorphism in the Pohorje nappe is Cretaceous, as shown by

U-Pb zircon ages from the gneisses of 91.9±0.5 Ma (Janák et al., 2008), a garnet Sm-Nd age (93–87 Ma) obtained from the gneisses and micaschists (Thöni, 2002), and by ca. 91 Ma garnet Sm-Nd and zircon U-Pb ages of eclogites (Miller et al., 2005). These ages are similar to those of Koralpe and Saualpe eclogite facies metamorphism (Thöni & Jagoutz, 1992; Thöni & Miller, 1996; Miller & Thöni, 1997; Thöni, 2002), which suggests that the Koralpe-Saualpe terrane and the Pohorje massif are part of the same subducted continental crust (Janák et al., 2004; 2008). Tertiary K-Ar mica ages (19–13 Ma) as well as apatite and zircon fission track ages (19–10 Ma) were obtained from the country rocks of eclogites and meta-ultrabasites in the Pohorje nappe (Fodor et al., 2002), which suggests that final exhumation occurred only in the Early to Middle Miocene. Upper Cretaceous (75 to 70 Ma) cooling ages were determined in the Koralpe area, the north-westward extension of the Pohorje nappe (Schuster et al., 2004), indicating that the Koralpe rocks were exhumed during the Upper Cretaceous. The main exhumation of the Pohorje nappe, from UHP to mid-crustal levels, most probably occurred during the Upper Cretaceous as well, and only the late stage of exhumation to the surface was achieved in the Miocene, by east- to north-east-directed low-angle extensional shearing leading to the core-complex structure of the Pohorje Mountains (Fodor et al., 2003). Protolith ages of Pohorje rocks are unknown, but as they occur in the same tectonic unit as the Koralpe and Saualpe rocks they probably underwent a similar stage of long-lived crustal extension or rifting accompanied by mafic magmatism in Permian-Triassic times (Thöni, 2002).

Other occurrences of ultramafic rocks that have been reported in the Eastern Alps (Gregurek et al., 1997; Meisel et al., 1997; Melcher et al., 2002) occur in different tectonic units that are not related to the continental subduction event.

2. Samples and analytical techniques

2.1. Sample locations and petrography

The ultramafic rocks within the SBUC are pervasively weathered and exposure is poor. Relatively unaltered material can only be found in fresh road cuts, at building sites and in a few small quarries. Five representative samples, four of which are strongly serpentinised harzburgites labelled SH-1-1, SH-123, SH-NO2 and SH-VO1, together with one partially serpentinised garnet lherzolite (GP-VI01; previously documented by Janák et al., 2006, as VI01-04) are investigated here (Table 1).

In harzburgites, remnants of olivine, orthopyroxene and Cr-spinel are locally preserved (Fig. 2A-F). Large orthopyroxene grains display abundant oriented exsolutions of Cr-spinel and sometimes clinopyroxene; they are variably replaced by serpentine, forming bastites, and amphibole. From the size of the bastites (up to 1 cm) we infer that the rocks were coarse-grained (Fig. 2A). The majority of the rock mass is replaced by a latest retrogressive stage assemblage coeval with serpentinisation involving serpentine minerals, chlorite, magnetite and talc. No clinopyroxene was preserved. Olivine is largely replaced by mesh-textured serpentine.

In garnet lherzolite (sample GP-VI01), the UHP metamorphic assemblage of garnet, olivine, Al-poor orthopyroxene, Al-poor clinopyroxene and Cr-spinel is variably replaced by amphibole (pargasite), Al-rich orthopyroxene and Al-spinel (see Janák et al., 2006, for a detailed description). Four stages of recrystallisation, from 1, a protolith (spinel peridotite) to 2, UHP metamorphism (garnet peridotite), 3, decompression, and 4, retrogression, have been identified based on analysis of reaction textures and mineral compositions (see Janák et al., 2006, for a detailed description).

2.2. Analytical techniques

Whole-rock chemical analyses were performed on ground powders prepared from hand pieces by crushing, grinding and milling in an iron jaw breaker and agate mills and mortars. The major elements Si, Al, Mg, Fe, Cr and Ca were determined by XRF after fusion with lithium metaborate (Geolab, Faculty of Geosciences, Utrecht University, The Netherlands). LOI was determined by stepwise heating of rock powder till 1000°C after a drying cycle at 150°C. Remaining major elements and minor and trace elements were analyzed at the Earth Science Centre (GVC) at Göteborg University, Sweden, by ICP-MS following the procedure described in Paulick et al. (2006). In summary, rock powders were digested in a hot HF-HNO_3 mixture and analyzed by solution ICP-MS (Agilent 7500) after drying and re-dissolution in dilute HNO_3. Rare earth elements, Ba, Y, Zr, Hf, Nb, Ta, Th, U were analyzed at a dilution factor (DF) of 500 to enable detection of the very low levels of these elements, whereas other trace elements were analyzed with a DF of ca. 3800. Standard reference materials UB-N, JB-2 and JGb-1 were measured to estimate accuracy. Our results were generally within 10% of recommended values. Visible chromite residues in the sample digests suggests that V and Zn values, which are enriched in chromites, are minimum estimates, but other elements should be unaffected.

Major element compositions of selected minerals were determined by SEM-EDS at the Earth Science Centre (GVC) at Göteborg University and by electron microprobe (CAMECA SX-100) at Dionýz Štúr Institute of Geology in Bratislava. Analytical conditions were 15 kV accelerating voltage and 20 nA beam current, with a peak counting time of 20 seconds and a beam diameter of 2-10 μm. Raw counts were corrected using a PAP routine. Mineral standards (Si, Ca: wollastonite, Na: albite, K: orthoclase, Fe: fayalite, Mn: rhodonite), pure element oxides (TiO_2, Al_2O_3, Cr_2O_3, MgO) and metals (Ni) were used for calibration.

3. Results

3.1 Major elements

The serpentinised harzburgites (Table 2, Fig. 3A, B) are characterized by high contents of MgO (41.5-44.3 wt.%[1]), high Mg# (0.86-0.91) and low contents of CaO and Al_2O_3 (0.15-0.9 and 0.7-1.2 wt.%, respectively). Na_2O (≤0.01 wt.%) and TiO_2 (≤0.02 wt.%) contents are very low. The serpentinised garnet peridotite sample has a very high Al_2O_3 content (7.8 wt.%), but CaO (2.5 wt.%) and Na_2O (0.2 wt.%) contents slightly below primitive mantle values. The sample is small and heterogeneous on hand-specimen scale (Fig. 2B), however, and therefore its composition is probably influenced by local variations in modal amounts of coarse-grained garnet (Fig. 2B). The composition falls in-between the harzburgites from the SBUC and garnet peridotites/pyroxenites from a nearby locality outside the SBUC (location 119, Modric, described in Janák et al., 2006); the latter are not serpentinised, however, and their relationship to the SBUC is not clear. Extensive serpentinisation of all the samples is indicated by their high water contents (loss on ignition LOI values), ranging from 10.6 to 13.8 wt%.

CIPW norm calculations following the calculation scheme of Niu (1997) classify the garnet-free rocks as harzburgites and the garnet-bearing one as lherzolite (Table 2). Although Niu's scheme is only valid for spinel peridotites, its application to the garnet-bearing sample is justified as garnet is of metamorphic origin and not part of the primary mineral assemblage (Janák et al., 2006). Normative *opx* values of all samples are relatively high, probably as a result of MgO loss during weathering, indicated by low MgO/SiO_2 ratios (see Section 4.1).

[1] All whole-rock data is reported on a volatile-free basis.

3.2 Trace elements

The harzburgites are rich in Ni (1900-2500 ppm) and Cr_2O_3 (0.30-0.36 wt.%). Nickel contents correlate positively with MgO contents. Cobalt shows little variation (96-110 ppm). Concentrations of all other trace elements are very low. Excellent correlations exist between Ti, Zr, Hf, Sc, V, Y, Th and Yb (Fig. 4), which are all incompatible elements that are immobile in fluids. These correlations suggest that the samples define a melt depletion (or refertilisation) trend. Concentrations of other incompatible elements (Ba, Sr, Rb, Cs, LREE, MREE, U, Pb) show little correlation and have likely been modified by various late-stage processes, which will be discussed later. One sample (SH-VO1) contains a very high amount of Pb (33 ppm), possibly related to the presence of sulphides, as Cu and Zn are also enriched in this sample.

Spider-diagram patterns, normalized to primitive mantle, are U-shaped, with very low contents of the moderately incompatible elements, but increasing concentrations of the more incompatible elements (Fig. 5). Some strong anomalies are present, the most apparent of which are positive U, Pb and Li anomalies and a negative Zr anomaly. REE contents of the harzburgites are low, with Lu_N ranging from 0.08-0.6. REE patterns are U-shaped, with strong depletions in MREE. The most depleted sample, SH-123, exhibits a small positive Eu anomaly (Eu*/Eu=2.0), whereas the other samples show weak to nearly invisible Eu anomalies. Two samples, SH-1-1 and SH-NO2, show small negative Ce anomalies (Ce*/Ce = 0.53 and 0.23, respectively). Y/Ho ratios are all suprachondritic (ca 1.1, except SH-NO2: 1.46). HREE patterns are positively sloped (Yb_N/Gd_N =1.2-4), consistent with considerable melt depletion. The garnet lherzolite has a weakly U-shaped pattern with a strong positive Eu anomaly (Eu/Eu*=2.3), and HREE contents similar to the harzburgites (Lu_N=0.44).

3.3. Mineral compositions

Remnants of original minerals can be found in the serpentinised harzburgites (Table 3). In sample SH-123 remnant olivine is Fo91.2 and has 0.44 wt% NiO. Orthopyroxene has high Mg# (0.912-0.923), low but variable Al_2O_3 (0.8-1.9 wt%) and low CaO (<0.3 wt%); it contains abundant oriented exsolutions of Cr-spinel (Cr# ~0.35) and occasionally Cpx exsolutions are observed (Mg# 0.95). Amphiboles replaces primary mantle minerals and occur as three varieties with different Mg#: tremolite (Mg# 0.96), pargasitic hornblende (0.91) and anthophyllite (0.89). The latter contains oriented exsolutions of ferrochromite. Hornblende is Cr-rich (ca. 1.5 wt% Cr_2O_3). Cr-spinel occurs as small inclusions in amphibole and large grains in the matrix. It has a wide range of compositions (Cr# 0.48-0.88, Mg# 0.18-0.51) with low TiO_2 contents (<0.2 wt%). Large grains have the highest Cr# and show complex exsolutions patterns indicative of subsolidus recrystallisation.

Sample SH-NO2 consists of mesh-textured serpentine after olivine and bastites; it has no remnants of original mantle minerals except Cr-spinel. Large homogenous spinel grains have a constant composition of Cr# 0.51 and Mg# 0.52, whereas other grains show zoning, becoming more Cr-rich and Mg-poor towards the rim (up to Cr# 0.84 and Mg# 0.27) and are overgrown by magnetite. All have low TiO_2 contents (0.06-0.3 wt.%). Few small amphiboles are present (pargasitic hornblende with Mg# 0.92 and 1.5 wt% Cr_2O_3, tremolite with Mg# 0.97).

Harzburgite SH-VO1 is characterized by relatively low Mg# of the minerals (olivine Fo85-88, orthopyroxene Mg# 0.86-0.88), consistent with the low whole rock Mg# of this sample (0.86). Orthopyroxene is poor in Al_2O_3 and CaO (1.1-1.5 and 0.2-0.5, respectively), and contains oriented exsolutions of Cr-spinel (Cr# ~0.4). Olivine contains 0.3 wt% NiO. Three varieties of amphibole with different Mg# replace primary mantle minerals: tremolite (Mg# 0.94), pargasitic hornblende (0.86) and anthophyllite (0.85). Hornblende is Cr-rich (ca. 1.0 wt%

Cr_2O_3). Cr-spinel grains are characterized by very high Cr# (0.85-0.90), low Mg# (0.14-0.16), and high TiO_2 (0.7-1.7).

No mineral data is available from sample SH-1-1.

The garnet lherzolite (GP-VI01; see also Janák et al., 2006) contains olivine remnants with Fo88-90 and ca. 0.3 wt% NiO. Remnants of pyrope-rich garnet (Mg# 0.76) with variable but low Cr contents (0.1-0.5 wt%) are preserved in garnet with lower Mg# (down to 0.64) and higher CaO contents (Fig. 2B). Some clinopyroxene (Mg# 0.90-0.94) is preserved. Orthopyroxene occurs with aluminous spinel as a breakdown product of garnet, in which case it is Al-rich (up to 2.5 wt.%), and as remnant primary mineral (Mg# 0.89-0.91) with lower Al_2O_3 (0.8-1.6 wt%). The latter contains abundant exsolutions of Cr-spinel and rare clinopyroxene. Pargasitic hornblende with Mg# 0.90 grows in coronas around garnet, it has highly variable Cr_2O_3 contents (0.1-1.7 wt%). Cr-spinels are often zoned, show a range of compositions (Mg# 0.46-0.58, Cr# = 0.35-0.52), and have low TiO_2 contents (<0.14 wt%). The compositions of olivine and Cr-spinel were used to estimate oxygen fugacities and equilibration temperatures of the samples following the method from Ballhaus et al. (1991). Mineral compositions of the samples SH-123, SH-NO2 and GP-VI01 indicate an oxidation state relative to the NNO buffer of -0.3 to +0.8, whereas sample SH-VO1 shows extremely high values of over three log units above NNO (Table 2). Closure temperatures are low (660-720°). As these are easily reset to lower temperatures (Barnes, 2000) they probably represent cooling of the hot mantle protolith down to UHP conditions rather than crystallisation temperatures, or even re-equilibration temperatures during greenschist to amphibolite-facies overprint. In addition, it is unclear to what extend serpentinisation affects oxidation states, as it may oxidize as well as reduce the rocks (Mevel, 2003; Frost and Beard, 2007). Therefore, we deem the oxidation states unreliable and will not discusse these further in the remainder of the manuscript.

4. Discussion

4.1. Geochemical effects of serpentinisation and alteration

Because the rocks from the SBUC are strongly serpentinised and all rocks in the Pohorje unit have suffered greenschist to amphibolite facies overprint (Janák et al., 2004; 2006), any resulting changes in their geochemical composition need to be evaluated before we can use that composition to make inferences about the tectonic origin and protoliths of the rocks. In general, most major elements, except Na, K and P, are regarded conservative during serpentinisation (e.g., Niu, 2004; Paulick et al., 2006). For trace elements it has been shown that alkalis, earth alkalis, LREE, Pb and U are variably sensitive to serpentinisation and alteration.

The harzburgites fall within the oceanic array (Niu, 2004) in $MgO/SiO_2 – Al_2O_3/SiO_2$ space (Fig. 3B). The oceanic array is parallel to the terrestrial array but offset to lower MgO/SiO_2 values, presumably due to loss of MgO during low-T sea floor weathering, not the serpentinisation process itself (Snow and Dick, 1995; Niu, 2004). We cannot constrain the timing of MgO loss in our samples, as the samples have clearly undergone late-stage weathering during and after exhumation. However, various orogenic ultramafics from Austria and Albania (Melcher et al., 2002; Pamić et al., 2002) from a variety of tectonic origins also plot below the terrestrial array, which suggests that weathering of continental rocks may have similar effects as sea-floor weathering.

We observe, however, that good correlations between many Yb and many trace elements and several major elements exist (Fig. 4), which argues against mobility of the elements. Therefore we feel confident that HREE and HFSE can be reliably used for determination of the (tectonic setting of the) protoliths.

4.2. History of the rocks: melting and metasomatism

The low trace-element contents of the serpentinised harzburgites suggest significant melt depletion of the protoliths. We modelled the extent of melting based on the REE contents of the rocks, using a non-modal fractional melting model with depleted MORB mantle (DMM, the source for MORB; Workman and Hart, 2005) as a starting composition under the assumption that melting took place in the spinel stability field (Fig. 7). The results show that the harzburgites can de derived from DMM by 15-29% melting. These degrees of melting are significantly higher than those commonly inferred for residual MOR mantle (e.g., Hellebrand et al., 2001; Niu, 2004), yet similarly depleted HREE values have been reported for abyssal peridotites from ODP Hole 209 (Paulick et al., 2006; Godard et al., 2008). HREE contents are inconsistent with melting in the garnet stability field, as the strong affinity of HREE for garnet would result in a much smaller spread in HREE contents. The Mg# of the rocks are slightly lower than expected for strongly melt-depleted residues, which is likely to be related to the afore-mentioned Mg-loss during weathering (Section 4.1).

HREE contents of the garnet lherzolite (GP-VI01) are also indicative of significant amounts (ca. 18%) of partial melting in the spinel stability field (garnet is of metamorphic origin during UHP conditions; Janák et al., 2006), which is at odds with the fertile major element composition of this sample. This points to refertilisation after melting, which will be discussed below.

The calculated melt depletions are broadly consistent with spinel compositions. It has been shown that in abyssal peridotites Cr# in spinel increase with the degree of melting, with a Cr# value of 0.5 being equivalent to 15-20% melting (Hellebrand et al., 2001). Significantly higher Cr#, up to 0.8, have been reported from spinels in supra-subduction zone mantle (e.g., Ozawa, 1994; Parkinson and Arculus, 1999) and layered mafic intrusions (Dick and Bullen,

1984; Barnes and Roeder, 2001). The garnet peridotite contains spinels with Cr# of 0.35-0.5, whereas the harzburgites are characterized by variable but high Cr# (0.45-0.9). The latter compositions, however, appear to be influenced by serpentinisation or later metamorphic overprint. Large homogenous grains in SH-NO2 have a constant composition of Cr# 0.51, whereas smaller grains are often zoned, becoming more Cr-rich towards the rims (up to 0.85; Fig. 6). Ferric iron contents increase as well, whereas Mg# decrease. This suggests an increase in oxidation state and a decrease in equilibration temperature, consistent with metamorphic overprint under amphibolite facies conditions (Barnes, 2000). Large homogenous spinels with similar relatively low Cr# are most likely to be representative of the protolith, but it remains difficult to assess to what extent they were modified by late-stage processes. The minimum Cr# of Cr-spinels from samples SH-123 (Cr# 0.48) and SH-NO2 (Cr# 0.51) are within the range of those from GP-VI01.

Spinels from harzburgite SH-VO1 all have very high Cr# (0.85-0.90) and are distinct from the other samples also because of their high TiO_2 contents (0.7-0.9 wt.%), a feature absent in typical subduction-zone related harzburgites (Dick and Bullen, 1984; Ishii et al., 1992). Similarly TiO_2-rich, high Cr# spinels have been found in abyssal plagioclase peridotites and dunites (Dick and Bullen, 1984) as well as in dunite channels from the Oman ophiolite (Kelemen et al., 1995). The high TiO_2 contents are interpreted to indicate equilibration with a melt phase of MORB composition (Kelemen et al., 1995). However, Fe^{3+} and Mg# of spinels from SH-VO1 are respectively much higher and lower than those from the above-mentioned settings. Mantle-xenoliths with strong metasomatic overprint by Fe-rich basaltic melts may carry Cr and TiO_2-rich spinels but are characterized by much higher Mg# as well (Ionov et al., 2005). Mafic layered intrusions and Alaskan-type ultramafics appear to have similar chromites (Barnes and Roeder, 2001), which points possibly to a cumulate origin of this sample, in accordance with its low Mg# and relatively low-Fo olivine (86.5). Alternatively,

the sample may have suffered melt infiltration, as a suite of chromites from melt-infiltrated layered harzburgites from the Miyamori ophiolite complex in Japan (Ozawa, 1994) show spinel compositions similar to those in SH-VO1. We conclude that spinel compositions of sample SH-VO1 are not related to the melting event and therefore its Cr# not indicative of the extent of melting.

In contrast to the HREE contents of the serpentinites, LREE and MREE contents differ significantly from patterns expected for a melting residue (Fig. 7). This points to late-stage modification of the samples (Hellebrand et al., 2002). With the exception of variable Ce and Eu-anomalies, L-MREE patterns of the harzburgites and lherzolite are parallel, which suggests the samples were affected by a similar metasomatic agent to different degrees. One explanation is that residual melt is preserved in the rocks, as all melt may not have been completely extracted from the residue. Only very small amounts of melt need to be left behind to cause significant changes in the residue, e.g., assuming a melt with La_N=20, then the amount of melt left in the residue needed to explain the observed La concentrations is only 0.3-2%. This will have a negligible effect on concentrations of major and moderately incompatible elements of the rocks. However, the metasomatic agent must have been enriched in LREE (La/Gd>1), whereas depleted harzburgites would produce LREE-depleted melts like N-MORB. It is, therefore, more likely that external melt has been added to the rock. We note that the L-MREE patterns of the serpentinites are similar to those of gabbroic dikes found within abyssal peridotites (Paulick et al., 2006). Similar patterns of LREE enrichment can also develop by chromatographic effects during porous flow, where the more incompatible elements travel faster through the melting column (Navon and Stolper, 1987), but this would lead to LREE patterns that vary with the extend of melt infiltration, a feature not observed in our samples. Niu (2004) observed a similar whole-rock LREE enrichment of abyssal peridotites which correlated with HFSE enrichment. The LREE enrichment was absent in

clinopyroxene grains, which pointed to diffuse grain-boundary infiltration of melt in the thermal boundary layer underneath the oceanic crust (Niu, 2004). Depleted harzburgites from the East Pacific Rise showed evidence of subsolidus veining, refertilisation and chromatographic fractionation, indicating that the various processes may operate at the same time (Hellebrand et al., 2002).

Additional constraints on the composition of the metasomatic agent can by derived from the behaviour of trace elements with partitioning coefficients during melting similar to those of the REE (e.g., Sr, Zr, Ti). We observe the following systematics: (1) Ti contents of the rocks are close to what would be expected for melting residues; (2) all but one sample have positive Sr anomalies, the most prominent of which also have the strongest positive Eu anomalies; (3) Zr is strongly depleted but still higher than expected based on partial melting modelling, whereas Nb and Th are strongly enriched compared to any expected melting residue similarly to LREE. The high Th and Nb argue against a dominant role of fluid metasomatism (Li and Lee, 2006), whereas the lack of TiO_2 enrichment can readily be explained by the relatively high concentration in the whole rock, so that small amounts of melt infiltration would not increase TiO_2 detectably. Any melt influx was probably not significant enough to alter the mineralogy of the harzburgites (i.e., cryptic metasomatism), but it most likely precipitated clinopyroxene in the garnet lherzolite (i.e., modal metasomatism).

Even though melts were probably the most important metasomatic agent, fluids may still have played a role. As mentioned above, two samples show positive Eu and Sr anomalies (SH-123 and GP-VI01), a feature commonly associated with plagioclase accumulation. Although we cannot discount the possibility that the garnet lherzolite has a plagioclase-bearing protolith, such a signature is unlikely to be preserved in depleted mantle residues, such as SH-123. Considerably stronger Eu anomalies were observed in abyssal peridotites altered by fluid-dominated serpentinisation (Paulick et al., 2006), whereas rock-dominated serpentinisation

resulted in less strong Eu anomalies and melt infiltration lead to little change. The Eu anomalies indicated that the fluids had probably interacted with gabbroic cumulates deeper in the crust underlying the serpentinite bodies (Paulick et al., 2006). We envision that a similar process may have influenced the Pohorje serpentinites, but it is important to point out that the timing and setting of serpentinisation plays an important role in the composition of the fluids. Serpentinisation of abyssal serpentinites takes place at the sea-floor and will be dominated by seawater, whereas serpentinisation in supra-subduction zone mantle will be controlled by fluids expelled from the slab, most likely seawater-like pore water from sediments in the fore arc and dehydration of minerals in deeper sections. The Pohorje ultramafics, however, must have been serpentinised during exhumation, as UHP conditions are above the stability field of serpentine (Ulmer and Trommsdorff, 1999) and petrographic evidence of an earlier low-*P* high-*T* stage of the ultramafic rocks (Janák et al., 2006) makes an earlier serpentinisation stage unlikely. Therefore, Pohorje serpentinites may show a crustal fluid signature, which could also explain the positive Eu and Sr anomalies.

We conclude that the SBUC rocks were formed by extensive melting (15-30%) in the spinel-stability field. Subsequent cryptic metasomatism resulted in partial refertilisation of the harzburgites, whereas the lherzolite probably underwent stronger modal metasomatism. Serpentinising fluids may have contributed to the trace element patterns as well, whereas during later amphibolite-greenschist facies overprint only the concentrations of several mobile elements were altered.

4.3. Tectonic setting of the protoliths

The Earth contains three main shallow mantle domains: sub-oceanic lithosphere, sub-continental lithosphere and supra-subduction zone mantle. Subcontinental lithosphere,

commonly observed as orogenic peridotite massifs and peridotite xenoliths from alkali basalts, is generally characterized by relatively fertile compositions (e.g., Jochum et al., 1989) with depleted harzburgites representing only a subordinate fraction. Only Archæan subcontinental rocks have a large proportion of depleted harzburgites, and have been found in some continental subduction zones (e.g., Western Gneiss Region, Norway; Spengler et al., 2006), but the Pohorje harzburgites miss other characteristics typical of cratonic peridotites, such as very high Cr# and Mg#, and, importantly, no Archæan basement rocks have been found elsewhere in the region. Spinel peridotite xenoliths from Kapfenstein, Austria, emplaced during Plio-Pleistocene rifting, have distinctly different compositions than the nearby Pohorje harzburgites (Kurat et al., 1980; Vaselli et al., 1996). It is therefore unlikely that the serpentinised harzburgites are former pieces of the subcontinental lithosphere. Strongly depleted mantle rocks are commonly observed as abyssal peridotites on the sea floor (e.g., Niu, 2004; Paulick et al., 2006) or as rocks from the sub-arc mantle (e.g., Parkinson et al., 1992; Parkinson and Arculus, 1999; Savov et al., 2007). However, distinguishing between these two tectonic settings purely on geochemical evidence is not straightforward for serpentinised rocks. We will now discuss a number of geochemical features in an attempt to pinpoint the tectonic setting of the rock protoliths, a summary of which is given in Table 4.

MgO/SiO_2 values. Low values below the terrestrial $MgO/SiO_2 – Al_2O_3/SiO_2$ array have been associated with serpentinites of oceanic affinity due to loss of MgO during low-T sea floor weathering (Snow and Dick, 1995; Niu, 2004). The SBUC harzburgites fall below the terrestrial array; it is, however, difficult to constrain the timing of MgO loss in our samples, as the samples have undergone late-stage weathering and metamorphic overprint. High MgO/SiO_2 values in Himalayan serpentinites, comparable to those from the Mariana forearc, lead Hattori and Guillot (2007) to postulate that such values are diagnostic of a supra-subduction zone (SSZ) origin, but similarly high MgO/SiO_2 values have recently been

reported for abyssal peridotites (ODP Leg 209; Paulick et al., 2006; Godard et al., 2008), which indicates that such signatures are not unique to SSZ settings. Therefore, we conclude that neither high nor low MgO/SiO_2 values are diagnostic of any particular setting in the absence of additional corroborating evidence.

Melt depletion. Systematic changes in parameters indicative of degree of melting, such as modal clinopyroxene content, Fo% of olivine, Al_2O_3 of orthopyroxene and Cr# of spinel, suggest an increasing degree of melt depletion of mantle peridotites from continents to passive margins to mature oceans to subduction zones (Bonatti and Michael, 1989). Compared to abyssal peridotites, which represent exposed pieces of upper mantle at oceanic ridges, Pohorje harzburgites fall within the most depleted part of the oceanic array defined by Niu (2004) but on average still less depleted than abyssal peridotites from ODP Leg 209 (Mid-Atlantic Ridge; Paulick et al. 2006). Arc xenoliths are usually strongly depleted by a combination of flux and decompression melting, which has been attributed to the melting rate of clinopyroxene being lower in hydrous peridotites, allowing for larger degrees of melting before clinopyroxene is exhausted from the residue (Bizimis et al., 2000). For example, peridotites from serpentinite seamounts in the Mariana forearc are characterized by very low whole-rock Ti and Y contents (10-25 ppm and 0.015-0.12 ppm, respectively), intermediate to high Cr# spinel (0.38-0.83) and steep HREE slopes (Y_N/Yb_N=0.12-0.40; Parkinson et al., 1992; Ishii et al., 1992). It appears that suites of abyssal peridotites are often characterized by a range of compositions, whereas those from SSZ settings are invariably strongly depleted. We conclude that the degree of melting of the SBUC is more consistent with an oceanic origin than a SSZ setting, as there is a considerable range in depletion parameters that overlap with abyssal peridotites, whereas no extreme values common in SSZ peridotites are observed.

Cr# of spinel. High Cr# are indicative of high degrees of melting (Dick and Bullen, 1984; Hellebrand et al., 2001) and values higher than 0.6 are usually restricted to subduction-related

rocks (Dick and Bullen, 1984). Cr# of spinels in our samples show a wide range of 0.35-0.9, which would be consistent with a SSZ setting for the SBUC. However, as discussed in Section 4.2., many Cr-spinels in the harzburgites show clear evidence of modification by late-stage processes, leading to an increase of Cr# by as much as 0.3 within a single grain (Fig. 6). If we take minimum Cr# (0.48-0.51) as most representative, all samples fall within the abyssal peridotite field, except for sample SH-VO1, in which Cr-spinels cannot be related to a melting event due to their high TiO_2 contents.

Li, U , Pb anomalies. Positive anomalies of Li, U and Pb are characteristic of hydrothermally altered ocean-floor peridotites since ocean water is strongly enriched in these fluid-mobile elements (Li and Lee, 2006). The SBUC harzburgites have high U contents, whereas the garnet lherzolite has a much lower U content, comparable to U contents of unaltered garnet peridotites from a locality outside the SBUC (Janák et al., 2006). This suggests serpentinisation may not be the cause of U enrichment of the harzburgites. Pb is enriched in all these rocks (high Pb/Ce ratios), as is Li. We note, however, that both Li and U contents of the harzburgites are significantly lower than most of the abyssal peridotites from Niu (2004). Textural evidence suggests that serpentinisation of rocks from the SBUC took place during exhumation after subduction to UHP conditions (Janák et al., 2006) and there is no evidence of an earlier serpentinisation event. Hence, serpentinisation took place but in the continental crust, not at the ocean floor. The origin of Li, U and Pb enrichment is therefore most likely of crustal origin although we cannot exclude hydrothermal modification during an earlier event in the history of the rocks.

Negative Ce anomalies. Negative Ce anomalies are rather ubiquitous in abyssal peridotites (Niu, 2004) and are attributed to seawater interaction, as deep seawater has a distinct negative Ce anomaly (Elderfield and Greaves, 1982). Also deep-sea sediments commonly have negative Ce anomalies, and are thought to have played a role in the genesis of some garnet

peridotites of SSZ setting and arc basalts (Neal and Taylor, 1989). They are, however, rarely observed in orogenic peridotites (e.g., Becker, 1996), but have been observed in some serpentinites in the Eastern Alps (Melcher et al., 2002). As similar negative Ce anomalies have been observed in several relatively fresh garnet peridotites from Pohorje (Janák et al., 2006) it is unlikely that the Ce anomalies are the result of serpentinisation. Therefore, the metasomatic agent that enriched the Pohorje peridotites in LREE was probably variably depleted in Ce. As materials with negative Ce anomalies can be found at the seafloor as well as in subduction zones we find the presence of Ce anomalies inconclusive as to the tectonic origin of the rocks.

Negative HFSE anomalies. The Pohorje peridotites show distinctly negative anomalies for Zr, but not for Nb and Ti (when compared to other refractory elements, such as Th). Negative HFSE anomalies are thought to be characteristic of SSZ mantle, as arc volcanics usually show HFSE depletions (Maury et al., 1992). The origin of HFSE depletion in SSZ mantle is still debated, but is often attributed to the low solubility of these elements in the aqueous fluids coming from the subducting slab or the presence of residual HFSE-bearing minerals in the slab or sub-arc mantle (Thirlwall et al., 1994). Pohorje serpentinites are not more depleted in HFSE than typical abyssal rocks, which argues against a SSZ setting, but as SSZ rocks without any such signature are also known (Ionov et al., 2007), the absence of such a signature is cannot be used to distinguish between different tectonic settings.

Fluid-mobile elements. Fluid-mobile elements are enriched in serpentinites in general, while certain elements such as As, Sb, Cs, Li and Pb are particularly enriched in SSZ settings (Hattori and Guillot, 2007; Savov et al., 2007). The serpentinites from Pohorje lack such as SSZ signature (Fig 8.). Serpentinising fluids in Pohorje were most likely of crustal origin, as serpentinisation occurred during exhumation, although it may even carry a signature of multiple fluid sources if the peridotitic protolith was already partially hydrated before

subduction. This may explain why Pohorje serpentinites have U contents similar to those of abyssal peridotites, and considerably higher than fore-arc serpentinites (Savov et al., 2007), but Cs enrichments more typical of crustal fluids.

In summary, the SBUC serpentinites lack any of the parameters typical of peridotites from SSZ settings, such as extreme melt depletion and fluid-mobile chalcophile element enrichment, and are too depleted to be derived from the sub-continental mantle. They do share many characteristics with depleted oceanic mantle, and we therefore conclude that this is the most likely protolith of the SBUC.

4.4. Implications for tectonic model of the Pohorje Mts.

Because of their simple mineralogy, depleted harzburgites will undergo little change during the pressure increase accompanying subduction. In highly depleted residues with Cr#>0.2 the stability field of Cr-spinel is expanded to >4 GPa (Klemme, 2004) and garnet may not form because CaO and Al_2O_3 contents are too low. In addition, the high speed of continental subduction and exhumation promotes the survival of metastable assemblages, and any evidence of an ultrahigh-pressure stage may be readily lost after extensive serpentinisation and metamorphic overprint. Therefore, it is impossible to state with certainty that the SBUC has experienced deep subduction based on the serpentinised harzburgites. However, the SBUC contains enclaves of rocks that have preserved evidence of a (U)HP stage, namely garnet peridotite sample GP-VI01, which recorded peak conditions of ca. 4 GPa and 900°C (Janák et al., 2006), and kyanite eclogites similar to those of nearby UHP locations (Janák et al., 2004; Vrabec, 2004). These confirm a high-pressure stage of the SBUC. Whether this piece of harzburgitic mantle became incorporated in the continental crust at an early stage, when it was still in the spinel stability field, or continued to be part of the mantle hanging

wall, dragged down by viscous coupling to the subducting crust, until exhumation started, is not clear.

The tectonic framework envisioned for the area gives several constraints (Fig. 9). After closure of the Meliata ocean by arc-continent collision, the system became locked because of the buoyancy of the underplating continental crust, and subduction continued several tens of kilometres northwards in purely intra-continental fashion (Janák et al., 2006), probably at the location of a former intracontinental rift zone which formed during the Permian (Janák et al., 2008). The first slab was extracted, probably after complete eclogitisation of the oceanic crust, and the second slab started exhuming in the void left by the first one (see Froitzheim et al., 2003, for a similar scenario for exhumation of the Adula nappe in the Central Alps). The Koralpe-Pohorje nappe comprises the second slab (Tenczer and Stüwe, 2003; Janák et al., 2004; Schmid et al., 2004).

This scenario implies that the top of the second slab was juxtaposed to consecutively continental crust, sub-continental lithosphere and the passive margin of the Meliata ocean comprising oceanic lithosphere. Therefore, the SBUC is most likely derived from the deeply subducted oceanic lithosphere attached to the first slab. In view of the paucity of ultramafic material in the less deeply subducted Koralpe-Saualpe region, it is conceivable that that part never was in contact with any mantle rocks. The maximum depth to which the SBUC was subducted is about 120 km (Janák et al., 2006). Garnet replacing spinel in some peridotites indicates that they were dragged down during subduction (Janák et al., 2006), probably after incorporation in the continental crust as the overlying mantle wedge was stagnant after the first slab became locked. This means that subduction of continental crust along the Meliata suture did not extend to greater depths than the spinel stability field.

Alternatively, the SBUC could be part of transitional mantle depleted during continental rifting, as the entire complex (Pohorje, Saualpe, Koralpe) was influenced by lithospheric

thinning and rifting in the Permian, with gabbroic intrusions in the lower crust and granitic intrusions and bimodal volcanism in the upper crust (Schuster et al., 2001; Janák et al., 2008). The rift became the site of the Cretaceous subduction zone, so that part of the rift became subducted (Pohorje), whereas the other part formed the hanging wall of the subduction zone, including the mantle parts. This mantle would carry the signatures of melt depletion and metasomatism during rifting, and part may have been dragged down during subduction to form the current SBUC.

The abundance in the Pohorje-Saualpe-Koralpe of Permian metagabbros and basalts (Thöni and Miller, 1996; Miller et al., 1997, 2005) supports such a rifting scenario, but the composition of the metabasalts, nearly exclusively N-MORB (Miller and Thöni, 1997; Sassi et al., 2004; our own unpublished data), is more typical of an oceanic or back-arc rift environment than of continental rifting, which is usually characterized by more enriched T- or E-MORB varieties or even alkaline rocks (e.g., Marroni et al., 1998; Desmurs et al., 2002; Dostal et al., 2001; Fodor et al., 1984; Kramer et al., 2003). Further study is needed to unravel the complex geological and tectonic history of the Pohorje region.

Conclusions

Serpentinised ultramafic rocks from the Slovenska Bistrica ultramafic complex in the Pohorje Mts, Slovenia, show evidence of significant melt depletion and variable amounts of later metasomatism. They probably represent parts of former oceanic mantle, as they share many mineralogical and geochemical characteristics with abyssal peridotites. Alternatively, the protolith was depleted and metasomatised in a continental rift zone. The rocks were incorporated in the subducting continental slab from the overlying mantle wedge during Eo-Alpine orogeny in the Pohorje region and subducted to UHP conditions, after which they were extensively serpentinised and overprinted by amphibolite-facies metamorphism during exhumation.

Acknowledgements. Constructive reviews by Frank Melcher and Gordon Medaris, Jr., are gratefully acknowledged and we thank Larissa Dobrzhinetskaya for editorial handling. This work was partially supported by research grants from the Swedish Council of Sciences (Vetenskapsrådet) for JdH, from the Slovak Grant Agencies APVV, No. 51-046105, and VEGA, No. 2/6092/26 for MJ, and by a L'OREAL Slovenia For Women in Science National Fellowship for MV.

References

Anders, E., Grevesse, N., 1989, Abundances of the elements: meteoritic and solar. Geochim. Cosmochim. Acta. 53, 197-214.

Ballhaus, C., Berry, R.F., Green, D.H., 1991, High pressure experimental calibration of the olivine-orthopyroxene-spinel oxygen geobarometer: implications for the oxidation state of the upper mantle. Contributions to Mineralogy and Petrology 107, 27-40

Barnes, S.J., 2000, Chromite in komatiites; II, Modification during greenschist to mid-amphibolite facies metamorphism. Journal of Petrology 41, 387-409

Barnes, S.J., Roeder, P.L.,, 2001, The range of spinel compositions in terrestrial mafic and ultramafic rocks. Journal of Petrology 42, 2279-2302

Becker, H., 1996, Crustal trace element and isotopic signatures in garnet pyroxenites and megacrysts from garnet peridotite massifs from Lower Austria. Journal of Petrology 37, 785–810.

Bizimis, M., Salters, V.J.M., Bonatti, E., 2000, Trace and REE content of clinopyroxenes from supra-subduction zone peridotites. Implications for melting and enrichment processes in island arcs. Chemical Geology 165, 67-85

Bonatti, E., Michael, P.J., 1989, Mantle peridotites from continental rifts to ocean basins to subduction zones. Earth and Planetary Science Letters 91, 297-311

Brueckner, H.K., Medaris, L.G., 2000, A general model for the intrusion and evolution of ‘mantle’ garnet peridotites in high-pressure and ultra-high-pressure metamorphic terranes. J. Metamorph. Geol. 18, 123–133

Carswell, D.A., 1986, The metamorphic evolution of Mg-Cr type Norwegian garnet peridotites. Lithos 19, 279-297

Desmurs, L., Müntener, O., Manatschal, G., 2002. Onset of magmatic accretion within a

magma-poor rifted margin: a case study from the Platta ocean– continent transition, eastern Switzerland. Contrib. Mineral. Petrol. 144, 365–382.

Dick, H.J.B., Bullen, T., 1984, Chromian spinel as a petrogenetic indicator in abyssal and alpine-type peridotites and spatially associated lavas, Contributions to Mineralogy and Petrology 86, 54–76.

Dostal J., Patoka F., Pin C. (2001) Middle/Late Cambrian intracontinental rifting in the central West Sudetes, NE Bohemian Massif (Czech Republic): geochemistry and petrogenesis of the bimodal metavolcanic rocks. Geological Journal 36, 1 - 17

Elderfield, H., Greaves, M.J., 1982, The rare earth elements in seawater. Nature 296: 214-219

Fodor, L., Balogh, K., Dunkl, I., 2003, Structural evolution and exhumation of the Pohorje-Kozjak Mts., Slovenia. Annales Universitatis Scientarum Budapestinensis, Sectio Geologica 35, 118–119.

Fodor, L., Jelen, B., Márton, E., 2002, Connection of Neogene basin formation, magmatism and cooling of metamorphics in NE Slovenia. Geologica Carpathica 53, 199–201.

Fodor, R.V., Vetter, S.K., 1984. Rift-zone magmatism: Petrology of basaltic rocks transitional from CFB to MORB, southeastern Brazil margin. Contributions to Mineralogy and Petrology 88, 307- 321

Froitzheim, N., Pleuger, J., Roller, S., Nagel, T., 2003, Exhumation of high- and ultrahigh-pressure metamorphic rocks by slab extraction. Geology 31, 925–928

Frost, B.R., Beard, J.S., 2007, On silica activity and serpentinization. Journal of Petrology 48, 1351-1368

Godard, M., Lagabrielle, Y., Alard, O., Harvey, J. (2008) Geochemistry of the highly depleted peridotites drilled at ODP Sites 1272 and 1274 (Fifteen-Twenty Fracture Zone, Mid-Atlantic Ridge): Implications for mantle dynamics beneath a slow-spreading ridge. Earth Planet. Sci. Lett. 267, 410-425

Gregurek, D., Abart, R., Hoinkes, G., 1997, Contrasting Eoalpine P-T evolutions in the southern Koralpe, Eastern Alps. Mineralogy and Petrology 60, 61-80

Guillot, S., Hattori, K.H., De Sigoyer, J., 2000, Mantle wedge serpentinisation and exhumation of eclogites: Insights from eastern Ladakh, northwest Himalaya. Geology 28 (3), 199-202

Hart, S.R., Zindler, A., 1986, In search of a bulk-Earth composition. Chemical Geology 57, 247-267

Hattori, K.H., Guillot, S., 2007, Geochemical character of serpentinites associated with high- to ultrahigh-pressure metamorphic rocks in the Alps, Cuba, and the Himalayas: Recycling of elements in subduction zones. Geochem. Geophys. Geosyst., 8, Q09010, doi:10.1029/2007GC001594, 27 p.

Hellebrand, E., Snow., J.E., Dick, H.J.B., Hofmann, A.W., 2001, Coupled major and trace elements as indicators of the extent of melting in mid-ocean-ridge peridotites. Nature 410, 677–681

Hellebrand, E., Snow, J. E., Hoppe, P., Hofmann A.W., 2002, Garnet-field melting and late-stage refertilization in "residual" abyssal peridotites from the Central Indian Ridge. Journal of Petrology 43, 2305-2338

Hinterlechner-Ravnik, A., Sassi, F.P., Visona, D., 1991a, The Austridic eclogites, metabasites and metaultrabasites from the Pohorje area (eastern Alps, Yugoslavia): 2. The metabasites and metaultrabasites, and concluding considerations. Rendiconti Fisiche Accademia Lincei 2, 175-190

Hinterlechner-Ravnik, A., Sassi, F.P., Visona, D., 1991a, The Austridic eclogites, metabasites and metaultrabasites from the Pohorje area (eastern Alps, Yugoslavia): 1. The eclogites and related rocks. Rendiconti Fisiche Accademia Lincei 2, 157–173

Ionov D.A., Chanefo I., Bodinier, J.-L., 2005, Origin of Fe-rich lherzolites and wehrlites from

Tok, SE Siberia by reactive melt percolation in refractory mantle peridotites. Contributions to Mineralogy and Petrology 150, 335-353

Ionov, D.A., Bruegmann, G., Seitz, H.-M., Lahaye, J., Woodland, A.B., 2007, Peridotite xenoliths from the andesitic Avacha volcano, Kamchatka – Any signatures of subduction metasomatism? (abstract) Goldschmidt Conference Abstracts, Cologne 2007, A430

Ishii, T., Robinson, P.T., Maekawa, H., Fiske R., 1992, Petrological studies of peridotites from diapiric serpentinite seamounts in the Izu-Ogasawara-Mariana forearc, Leg 1251. In: Fryer, P., Pearce, J.A., Stokking, L.B. (Eds.) Proceedings of the Ocean Drilling Program, Scientific Results, Vol. 125, pp. 445-485

Janák, M., Froitzheim, N., Lupták, B., Vrabec, M., Ravna, E.J.K., 2004, First evidence for ultrahigh-pressure metamorphism of eclogites in Pohorje, Slovenia: Tracing deep continental subduction in the Eastern Alps. Tectonics 23, TC5014, doi:101029/ 2004TC001641

Janák, M., Froitzheim, N., Vrabec, M., Krogh Ravna, E.J.K., De Hoog, J.C.M., 2006, Ultrahigh-pressure metamorphism and exhumation of garnet peridotite in Pohorje, Eastern Alps. Journal of Metamorphic Geology 24, 19–31

Janák, M., Cornell, D., Froitzheim, N., De Hoog, J.C.M., Broska, I., Vrabec, M., 2008, Metamorphic evolution of kyanite-garnet gneisses from the HP/UHP terrane, Pohorje Mountains (Eastern Alps, Slovenia): zircon ion microprobe dating and trace element distribution, *P-T* conditions, implications for deep subduction and exhumation of a coherent continental crust. Submitted manuscript to Journal of Metamorphic Geology.

Jochum, K. P., McDonough, W. F., Palme, H., Spettel, B., 1989, Compositional constraints on the continental lithospheric mantle from trace elements in spinel peridotite xenoliths. Nature 340, 548-551

Kelemen, P.B., Shimizu, N., Salters, V.J.M., 1995, Extraction of mid-ocean-ridge basalt from

the upwelling mantle by focused flow of melt in dunite channels. Nature 375, 747-753

Klemme, S., 2004. The influence of Cr on the garnet-spinel transition in the Earth's mantle: experiments in the system MgO-Cr_2O_3-SiO_2 and thermodynamic modelling. Lithos 77, 639-646.

Kramer J., Abart, R., Müntener, O., Schmid, S.M., Stern, W., 2003, Geochemistry of metabasalts from ophiolitic and adjacent distal continental margin units: Evidence from the Monte Rosa region (Swiss and Italian Alps). Swiss Bulletin of Mineralogy and Petrology 83, 217-240

Kurat, G., Palme, H., Spettel, B., Baddenhausen, H., Palme, C., Wänke, H., 1980, Geochemistry of ultramafic xenoliths from Kapfenstein, Austria. Evidence for a variety of upper mantle processes. Geochimica Cosmochimica Acta 44, 45–60

Li, Z-X. A, Lee, C-T. A., 2006, Geochemical investigation of serpentinised oceanic lithospheric mantle in the Feather River Ophiolite, California: Implications for the recycling rate of water by subduction. Chemical Geology 235, 161-185

Liou, J.G., Zhang, R.Y., 1998. Petrogenesis of an ultrahigh-pressure garnet-bearing ultramafic body from Maowu, Dabie Mountains, east-central China. The Island Arc 7, 115–134

Marroni, M., Molli, G., Montanini, A., Tribuzio, R., 1998, The association of continental crust rocks with ophiolites in the Northern Apennines (Italy): implications for the continent-ocean transition in the Western Tethys. Tectonophysics 292, 43-66.

Maury, R. C., Defant, M.J., Joron, J.-L., 1992, Metasomatism of the sub-arc mantle inferred from trace elements in Philippine xenoliths, Nature 360, 661–663.

McDonough, W.F., Sun, S., 1995, The composition of the Earth. Chemical Geology, 120, 223–253

Medaris, L.G., 2000, Garnet peridotites in Eurasian high-pressure and ultrahigh-pressure terranes: a discovery of origins and thermal histories. In: Ernst, W.G., Liou, J.G. (Eds.),

UHP Metamorphism and Geodynamics in Collision Type Orogenic Belts. Boulder, CO: Geological Society of America, pp. 57–73

Medaris, L.G., Carswell, D.A., 1990, Petrogenesis of Mg–Cr garnet peridotites in European metamorphic belts. In: Carswell, D.A. (Ed.), Eclogite Facies Rocks. Blackie, Glasgow London, pp. 260–290.

Medaris, L.G., Wang, H.F., Misar, Z., Jelinek, E., 1990, Thermobarometry, diffusion and cooling rates of crustal garnet peridotites- 2 examples from the Moldanubian Zone of the Bohemian Massif. Lithos 25, 189–202.

Meisel, T., Melcher, F., Tomascak, P., Dingeldey, C., Koller, F., 1997, Re-Os isotopes in orogenic peridotite massifs in the Eastern Alps, Austria. Chemical Geology 143, 217-229

Melcher, F., Meisel, T., Puhl, J., Koller, F., 2002, Petrogenesis and geotectonic setting of ultramafic rocks in the Eastern Alps: constraints from geochemistry. Lithos 65, 69–112

Mevel, C. (2003) Serpentinization of abyssal peridotites at mid-ocean ridges. Comptes Rendus Geoscience 335, 825-852

Miller, C., Thöni, M., 1997, Eo-alpine eclogitisation of Permian MORB-type gabbros in the Koralpe (eastern Alps, Austria): new geochronological, geochemical and petrological data. Chemical Geology 137, 283–310

Miller, C., Mundil, R., Thöni, M., Konzett, J., 2005, Refining the timing of eclogite metamorphism: a geochemical, petrological, Sm-Nd and U-Pb case study from the Pohorje Mountains, Slovenia (Eastern Alps). Contributions to Mineralogy and Petrology 150, 70–84.

Mioč, P., Žnidarčič, M., 1977, Geological map of SFRJ 1:100 000, Sheet Slovenj Gradec. Geological Survey, Ljubljana, Federal Geological Survey, Beograd.

Navon, O., Stolper, E., 1987, Geochemical consequences of melt percolation: The upper mantle as a chromatographic column. Journal of Geology 95, 285-307.

Neal, C.R., Taylor, L.A., 1989, Negative Ce anomaly in a peridotite xenolith from Malaita, Solomon Islands: Evidence for crustal recycling into the mantle or mantle metasomatism? Geochimica Cosmochimica Acta 53, 1035-1040.

Niu, Y., 1997, Mantle melting and melt extraction processes beneath ocean ridges: evidence from abyssal peridotites. Journal of Petrology 38, 1047–1074.

Niu, Y., Hékinian, R., 1997, Basaltic liquids and harzburgitic residues in the Garrett transform: a case study at fast-spreading ridges. Earth and Planetary Science Letters 146, 243–258

Niu, Y, 2004, Bulk-rock major and trace element compositions of abyssal peridotites: implications for mantle melting, melt extraction and post-melting processes beneath mid-ocean ridges. Journal of Petrology 45, 2423–2458

Ozawa, K., 1994, Melting and melt segregation in the mantle wedge above a subduction zone; evidence from the chromite-bearing peridotites of the Miyamori ophiolite complex, northeastern Japan. Journal of Petrology 35, 647-678

Pamić, J., Tomljenović, B., Balen, D., 2002, Geodynamic and petrogenetic evolution of Alpine ophiolites from the central and NW Dinarides: an overview. Lithos 65, 113–142

Parkinson, I.J., Arculus, R. J., 1999, The redox state of subduction zones: Insights from arc-peridotites, Chemical Geology 160, 409–423.

Parkinson, I.J., Pearce, J.A., Thirlwall, M.F., Johnson, K.T.M., Ingram, G., 1992, Trace elements geochemistry of peridotites from the Izu-Bonin-Mariana forearc, Leg 125. In: Fryer, P., Pearce, J.A., Stokking, L.B. (Eds.) Proceedings of the Ocean Drilling Program, Scientific Results, Vol. 125, pp. 487-506

Paulick, H., Bach, W., Godard, M., De Hoog, J.C.M., Suhr, G., Harvey, J., 2006, Geochemistry of abyssal peridotites (Mid-Atlantic Ridge, 15°20′N, ODP Leg 209): Implications for fluid/rock interaction in slow spreading environments. Chemical Geology

234, 179–210

Ravna E.J.K., Kullerud, K., Ellingsen E., 2006, Prograde garnet-bearing ultramafic rocks from the Tromsø Nappe, northern Scandinavian Caledonides. Lithos 92, 336–356

Sassi, R., Mazzolli, C., Miller, C., Konzett, J., 2004, Geochemistry and metamorphic evolution of the Pohorje Mountain eclogites from the easternmost Austroalpine basement of the Eastern Alps (Northern Slovenia). Lithos, 78, 235–261.

Savov, I.P., Ryan, J.G., D'Antonio, M., Fryer, P., 2007, Shallow slab fluid release across and along the Mariana arc-basin system: Insights from geochemistry of serpentinized peridotites from the Mariana fore arc. Journal of Geophysical Research 112, B09205, doi:10.029/2006JB004749

Schmid, S.M., Fügenschuh, E., Kissling, E., Schuster, R., 2004, Tectonic map and overall architecture of the alpine orogen. Eclogae Geologicae Helvetiae 97, 93–117

Schuster., R., Koller, F, Hoeck, V., Hoinker, G., Bousquet, R., 2004, Explanatory notes to the map: Metamorpic structure of the Alps – Metamorphic evolution of the Eastern Alps. Mitteilungen der Österreichischen Mineralogischen Gesellschaft 149, 175–199

Schuster, R., Scharbert, S., Abart, R. & Frank, W., 2001, Permo-Triassic extension and related HT/LP metamorphism in the Austroalpine - Southalpine realm. Mitteilungen der Gesellschaft der Geologie- und Bergbaustudenten in Österreich 44, 111-141

Snow, J.E., Dick, H.J.B., 1995, Pervasive magnesium loss by marine weathering of peridotite. Geochimica Cosmochimica Acta 59, 4219–4235

Spengler, D., Van Roermund, H.L.M., Drury, M.R., Ottolini, L., Mason, P.R.D., Davies, G.R., 2006, Deep origin and hot melting of an Archaean orogenic peridotite massif in Norway. Nature 440, 913-917

Sun, S.S., McDonough, W.F., 1989, Chemical and isotopic systematics of oceanic basalts; implications for mantle composition and processes. In: Saunders, A.D. Norry, M.J. (Eds.)

Magmatism in the ocean basins. Geological Society of London, London, pp. 313-345

Tenczer, V., Stüwe, K., 2003, The metamorphic field gradient in the eclogite type locality, Koralpe region, Eastern Alps. Journal of Metamorphic Geology 21, 377–393

Thirlwall, M. F., Smith, T. E., Graham, A. M., Theodorou, N., Hollings, P., Davidson, J. P., Arculus, R. J., 1994, High field strength element anomalies in arc lavas; source or process? Journal of Petrology 35(3), 819-838

Thöni, M., Jagoutz, E., 1992, Some new aspects of dating eclogites in orogenic belts: Sm-Nd, Rb-Sr, and Pb-Pb isotopic results from the Austroalpine Saualpe and Koralpe type locality (Carinthia/Styria, southeastern Austria). Geochimica Cosmochimica Acta 56, 347–368

Thöni, M., 2002, Sm-Nd isotope systematics in garnet from different lithologies (Eastern Alps): age results, and an evaluation of potential problems for garnet Sm-Nd chronometry. Chemical Geology 185, 255–281.

Thöni, M., Miller, C., 1996, Garnet Sm-Nd data from the Saualpe and the Koralpe (Eastern Alps, Austria): chronological and P-T constraints on the thermal and tectonic history. Journal of Metamorphic Geology 14, 453–466.

Ulmer, P., Trommsdorff, V., 1999, Phase relations of hydrous mantle subducting to 300 km. In: Fei, Y.-W., Bertka, C., Mysen, B.O. (Eds) Mantle Petrology: Field Observations and High Pressure Experimentation: a Tribute to Francis R. (Joe) Boyd. Geochemical Society, Special Publications 6. pp. 259–281

Vaselli, O., Downes, H., Thirlwall, M. F., Vannucci R., Coradossi, N., 1996, Spinel-peridotite xenoliths from Kapfenstein (Graz Basin, Eastern Austria): a geochemical and petrological study. Mineralogy and Petrology 57, 23-50

Visona, D., Hinterlechner-Ravnik, A., & Sassi, F. P., 1991, Geochemistry and crustal P-T polymetamorphic path of the mantle-derived rocks from the Pohorje area (Austrides, Eastern Alps, Slovenia). Mineralia Slovaca, **23**, 515-525.

Vrabec, M., 2004, High-pressure to ultrahigh-pressure metamorphism of Pohorje eclogites. Unpublished M.Sc. Thesis. Faculty of Natural Sciences and Engineering, University of Ljubljana, Slovenia.

Vrabec, M., 2007, Petrology of ultrahigh-pressure metamorphic rocks from Pohorje. Unpublished Ph.D. Thesis. Dept. of Geology, University of Ljubljana, Slovenia.

Wood, B.J., Blundy, J.D., 1997. A predictive model for rare earth element partitioning between clinopyroxene and anhydrous silicate melt. Contributions to Mineralogy and Petrology 129, 166-181.

Workman, R. K., Hart, S. R., 2005, Major and trace element composition of the depleted MORB mantle (DMM), Earth and Planetary Science Letters 231, 53-72

Yang, J.-J., Jahn, B.-M., 2000, Deep subduction of mantle-derived garnet peridotites from the Su-Lu UHP metamorphic terrane in China. Journal of Metamorphic Geology 18, 167–180

Yuan, H., Gao, S., Rudnick, R.L.. Jin, Z., Liu, Y., Puchtel, I.S., Walker, R.J., Yu, R., 2007, Re–Os evidence for the age and origin of peridotites from the Dabie–Sulu ultrahigh pressure metamorphic belt, China. Chemical Geology 236, 323–338

Figure captions

Figure 1. Simplified geological map of the southwest corner of the Pohorje Mountains (modified from Mioč and Žnidarčič, 1977, with updates by F. Kirst and S. Sandmann, University of Bonn) showing the location of the Slovenska Bistrica Ultramafic Complex (SBUC) and sampling localities. Inset shows location of Slovenia and Pohorje Mountains; gray rectangle represents geological map area.

Figure 2. (A) Photograph of surface of serpentinite hand specimen SH-VO1 showing coarse grained texture and presence of bastites (foliated mass of serpentine minerals replacing orthopyroxene, example indicated by arrow). (B) Photograph of cut surface of garnet peridotite hand specimen GP-VI01 showing coarse-grained streaky garnets (example indicated by arrow) in matrix of dominantly serpentine. (C) BSE image of amphibole replacing serpentinised mantle assemblage (SH-123). Its composition is anthophyllite (Ant), where it replaces bastite (Bas); it contains Cr-spinel exsolutions oriented along the same plane as the bastite. Tremolite (Trem) replaces the serpentinite matrix. (D) BSE image of large orthopyroxene grain showing oriented exsolutions of clinopyroxene and Cr-spinel needles and blebs (GP-VI01). (E) BSE image of remnants of olivine in serpentine matrix (SH-VO1). (F) Large Cr-spinel grain (Cr) in matrix of tremolite and serpentine (SH-VO1).

Figure 3. (A) CaO-MgO plot showing the composition of serpentinised ultramafic rocks (this study) compared to other HP-UHP mafic and ultramafic rocks from Pohorje (our unpublished data, descriptions of the rocks can be found in Janák et al., 2004, 2006). Abyssal peridotites (Niu, 2004) are plotted for comparison; also indicated are compositions of Depleted MORB Mantle (DMM; Workman and Hart, 2005)

and Primitive Mantle (PM; McDonough and Sun, 1995). (B) MgO/SiO_2 - Al_2O_3/SiO_2 (B) plots. The terrestrial array is a compilation of subcontinental peridotites (Hart and Zindler, 1986) and represents a melt depletion trend. Abyssal peridotites (Niu, 2004) plot offset to lower MgO/SiO_2 values because of weathering at the seafloor (Snow and Dick, 1995). Pohorje harzburgites fall towards the most depleted end of the array, but suffered Mg loss. The serpentinised lherzolite must have undergone significant refertilisation.

Figure 4. Variation diagrams of various trace elements against Yb of serpentinites from Pohorje. For the harzburgites, good correlation exists between Yb and Mg, Al, Sc, Cr, Th and Zr, whereas La and Rb show less good correlations. The correlation often breaks down for the lherzolite sample. For comparison the abyssal serpentinites from Niu (2004) are indicated in light gray symbols.

Figure 5. Trace-element spider diagram of Pohorje serpentinites normalized to primitive upper mantle (values from Sun and McDonough, 1989) with element order after Li and Lee (2006). The field of abyssal peridotites (Niu, 2004) and the composition of DMM (Workman and Hart, 2005) are plotted for comparison. See text for discussion.

Figure 6. Diagram of Mg# ($100\times Mg/(Mg+Fe^{2+})$) vs. Cr# ($100\times Cr/(Al+Cr)$) for Cr-spinel grains of selected serpentinites. Compositional fields are compiled from literature data by Dick et al. (1984) and Barnes and Roeder (2001). The majority of our grains have Cr# between 35 and 65, and fall on the same trend as Alpine-type peridotites from the Alps (Dick et al., 1984), which is offset to lower Mg# than Alpine-type peridotites from elsewhere. Some grains with low Cr# are found in coronas around garnet. Several spinels with very high Cr# in the harzburgites are probably the result of metamorphic overprint. For example, one zoned crystal from

SH-NO2 (dotted squares) shows nearly the whole compositional range of chromites in harzburgites, with highest Cr# near the rim.

Figure 7. Rare-earth element patterns normalized to chondrite. All patterns are U-shaped, indicative of melt depletion followed by metasomatism. Note the positive Eu anomalies in two samples and the negative Ce anomalies in two other samples. For comparison are indicated the composition of depleted MORB mantle (DMM; Workman and Hart, 2005) and melting curves by assuming non-modal fractional melting of a source of DMM composition in the spinel stability field. The extent of melting in the Pohorje peridotites varies from 15-30%. Modal composition of the source rock were as follows: cpx 0.13, opx 0.30, sp 0.02, ol 0.55; and melting reaction was 46.4 cpx + 68.1 opx + 4.8 sp = 19.3 ol + 100 melt (from Niu and Hékinian, 1997). $D_{REE/melt}$ values (La 0.016, Ce 0.024, Pr 0.034, Nd 0.045, Sm 0.068. Eu 0.077, Gd 0.088, Tb 0.095, Dy 0.102, Ho 0.109, Er 0.115, Tm 0.122, Yb 0.129, Lu 0.133) are from Niu and Hékinian (1997) except for La-Nd that were calculated from the clinopyroxene-melt lattice strain model by Wood and Blundy (1997). Chondrite values after Anders and Grevesse (1989).

Figure 8. Spider plot of fluid-mobile elements compared to other elements listed in order of melt compatibility after Hattori et al. (2007). Our data compares well with the fields of Alpine and Cuban serpentinites, and lack evidence for interaction with suprasubduction-zone fluids as do Himalayan serpentinites.

Figure 9. Tectonic scenario modified from Janák et al. (2006). Hypothetical cross-section of the Austroalpine orogen at c. 100 to 90 Ma. The crustal units currently representing Pohorje are deeply buried in an intra-Austroalpine subduction zone. The SBUC was incorporated from the deeper oceanic mantle part of the overlying mantle wedge or from mantle from a failed rift zone along which subduction of the

Pohorje slab started, and then carried down to UHP depth. Thick dashed lines indicate transition between different mantle domains (subcontinental and oceanic mantle). Exhumation was accommodated by later extraction of the Upper Central Austroalpine (UCA) lower crustal and mantle wedge. The dashed line delineates the extracted wedge. LA = Lower Austroalpine; UCA = Upper Central Austroalpine; LCA = Lower Central Austroalpine; SSZ = supra-subduction zone mantle; SLM = subcontinental lithospheric mantle; SOM = subducted oceanic mantle.

Insets show schematic view of slab extraction scenario and exhumation mechanism of Pohorje rocks after Janák et al. (2006).

Tables

Table 1. Sample locations and description

sample	type [a]	location	GPS	description
GP-VI1	SLh	Visole	46.408N 15.524E	Garnet lherzolite, partly serpentinised with relics of Gt, Ol, Opx, Cpx, Cr-spinel and sulphides (see Janák et al., 2006, for a detailed description)
SH-123	SHz	Markuž quarry	46.404N 15.493E	Serpentinised harzburgite with relics of Opx, Ol and Cr-spinel. Exsolutions of Cpx and Cr-sp from Opx. Amphiboles (hornblende, tremolite, anthophyllite) replacing serpentinised mantle minerals.
SH-NO2	SHz	Novak [b]	46.418N 15.529E	Strongly serpentinised harzburgite with relics of Cr-spinel, some amphibole (hornblende, tremolite)
SH-1-1	SHz	near Visole	46.408N 15.534E	Serpentinised harzburgite with relics of Ol, Cr-spinel and Opx.
SH-VO1	SHz	same as SH-1-1	same as SH-1-1	Coarse-grained serpentinised harzburgite with abundant relics of olivine, Opx and Cr-spinel. Amphiboles (hornblende, tremolite, anthophyllite). Sulphide-bearing. Cr-spinel exsolutions in Opx.

[a] SLh = serpentinised garnet lherzolite, SHz = serpentinised spinel harzburgite; [b] along road, not in situ

Table 2. Major and trace element compositions of serpentinites from Pohorje

wt.% [a]	**GP-VI01**	**SH-123**	**SH-NO2**	**SH-1-1**	**SH-VO1**	**UB-N** [g]
type	SLh	SHz	SHz	SHz	SHz	ANRT
SiO_2	42.33	45.09	46.47	45.11	42.43	45.29
TiO_2	0.031	0.0036	0.0053	0.018	0.018	0.091
Al_2O_3	7.87	0.67	0.83	1.24	1.06	3.17
Cr_2O_3	0.25	0.30	0.35	0.34	0.36	0.35
Fe_2O_3 [b]	9.51	9.38	8.70	9.22	13.37	9.48
MnO	0.133	0.115	0.081	0.096	0.183	0.152
MgO	34.73	44.46	43.26	44.33	41.42	41.16
CaO	2.52	0.50	0.39	0.15	0.88	1.45
Na_2O	0.193	0.0076	0.0065	0.0027	0.0109	0.126
K_2O	0.028	0.0055	0.0083	0.0079	0.0075	0.0172
P_2O_5	0.0043	0.0041	0.0097	0.0198	0.0053	0.0089
Total	97.62	100.32	99.95	100.42	99.76	101.26
LOI [c]	10.58	13.81	12.87	12.44	11.95	10.69
Mg#	0.878	0.904	0.908	0.905	0.860	
Cr#	0.02	0.23	0.22	0.15	0.19	
CIPW norm [d]						
ol	39.4	64.6	55.4	63.3	70.4	
opx	40.1	30.4	39.9	32.4	22.8	
cpx	14.7	2.4	2.0	0.7	4.2	
ppm [e]						
Li	29.0	3.63	1.44	1.94	3.13	29.4
Sc	5.5	5.2	6.2	9.0	12.6	15.9
V	23.8	11.1	23.9	30.9	46.3	84
Co	107	121	117	120	121	113
Ni	1790	2430	2470	2240	1880	1740
Cu	25.3	0.77	1.99	1.18	12.8	31
Zn	46.1	31.0	36.3	38.5	67.7	95
As	0.64	2.19	0.99	6.38	0.71	9.7
Sb	0.055	0.057	0.016	0.091	0.260	na
Sr	18.6	3.79	2.18	0.48	3.14	6.5
Y	0.65	0.047	0.268	0.290	0.49	2.79
Zr	0.64	0.038	0.055	0.23	0.30	3.8
Ba	50.2	2.51	2.54	1.26	2.63	31.5
Pb	0.60	0.14	0.54	0.22	33.8	11.5
ppb [e]						
Rb	1206	284	51	64	272	2880
Nb	179	70	21	25	60	55
Cs	658	540	33	29	136	8530
La	228	14.4	121	51	81	319
Ce	583	39	59	58	190	794
Pr	78	5.8	33	13.4	25.8	120
Nd	388	27.3	157	59	115	616
Sm	88	6.1	31	15.6	32	216
Eu	76	3.9	11.4	6.0	13.5	82.6
Gd	114	5.5	31	19.9	41	329
Tb	17	0.84	3.8	3.7	8.1	63.6
Dy	117	5.7	25.6	33	63	449
Ho	20.9	1.52	6.6	9.4	16.3	99.3
Er	66	5.8	21.7	37	60	300
Tm	11.5	1.21	3.8	7.6	11.9	46.6
Yb	79	12.2	30	68	101	320
Lu	13	2.43	5.5	12.8	19.0	48.3
Hf	37	1.10	1.91	7.6	9.4	133
Ta	na [f]	18.8	23.4	17.8	19.2	17.6
Th	34	1.10	2.75	5.7	14.1	67
U	5.2	23	118	157	116	73

[a] Major elements in wt.% oxide (recalculated to volatile-free rock composition) by XRF except TiO_2, Na_2O, K_2O and P_2O_5 by ICP-MS. [b] All Fe reported as Fe_2O_3. [c] LOI = loss on ignition, values given are from before normalization of major elements to volatile-free compositions. [d] CIPW norms calculated following the scheme by Niu (1997) [e] All trace elements by ICP-MS, recalculated to volatile-free rock composition. [f] na = not analyzed. [g] UB-N is a serpentinite reference material provided by ANRT, France

Table 3. Composition of selected minerals by EDS-SEM and electron microprobe

	SH-123							SH-NO2				SH-VO1						GP-VI01						
	Ol	Opx	Cpx exsol	Cr	Hbl	Antp	Trem	Serp	Cr	Hbl	Trem	Ol	Opx	Cr	Antp	Hbl	Trem	Ol	Opx	Cpx	Grt	Cr	Hbl	Trem
SiO_2	41.32	57.23	55.70	0.12	45.87	60.65	56.84	39.11	0.10	46.50	59.14	40.03	56.04	0.09	59.35	46.92	58.53	40.65	57.20	52.95	42.22	0.12	46.04	58.03
TiO_2	<0.01	<0.01	0.07	0.09	0.07	0.01	0.06	0.10	0.06	0.08	0.01	<0.01	0.02	1.69	<0.01	0.07	0.02	0.01	<0.01	<0.01	0.04	0.12	0.17	0.01
Al_2O_3	<0.05	1.30	0.75	22.81	12.71	<0.05	2.08	1.21	25.55	12.55	0.72	<0.05	1.15	2.47	0.13	10.58	0.18	<0.05	1.71	4.87	23.47	25.76	14.33	1.22
Cr_2O_3	<0.01	0.33	0.63	41.27	1.51	0.07	0.42	1.52	39.02	1.49	0.37	<0.01	0.27	33.55	<0.01	1.18	0.13	0.01	<0.01	0.16	0.51	40.63	1.37	0.10
Fe_2O_3 [a]				4.01					4.59					30.04										
FeO	8.70	5.90	1.83	19.46	3.35	7.00	1.65	7.33	18.47	3.14	1.57	12.96	8.09	29.21	9.66	5.33	2.74	11.29	6.86	3.36	10.47	20.86	3.62	1.93
MnO	0.15	0.18	0.06	0.27	0.15	0.23	0.01	0.01	0.33	0.04	0.04	0.17	0.19	0.49	0.46	0.09	0.10	0.14	0.09	0.09	0.39	0.34	0.03	0.05
MgO	50.84	35.37	19.41	10.02	19.35	30.44	23.47	35.87	11.22	19.54	24.43	46.77	32.94	2.53	28.49	18.89	23.63	48.53	34.06	17.65	18.75	10.22	18.48	23.21
CaO	<0.01	0.30	22.68	0.12	12.39	0.56	13.27	0.03	<0.01	12.78	13.02	<0.01	0.25	0.02	0.67	12.31	12.69	<0.01	0.30	21.32	5.88	0.02	12.59	13.45
Na_2O	<0.10	<0.10	0.20		2.45	<0.10	0.47	<0.10		2.59	0.12	<0.10	<0.10		<0.10	2.32	0.35	<0.10	<0.10	0.29	<0.10		1.68	<0.10
K_2O	<0.01	<0.01	<0.01		0.13	<0.01	0.04	<0.01		0.08	<0.01	<0.01	<0.01		0.03	<0.01	<0.01	<0.01	0.01	0.01	0.01		0.08	0.01
NiO	0.44	0.11	0.07	0.09	<0.01	0.11	0.11	0.10	0.08	0.09	0.05	0.29	0.09	0.16	<0.01	0.07	0.11	0.30				0.08		
ZnO				0.40				0.03	0.58					0.29								0.35		
V_2O_3				0.35				0.05	0.20					0.64								0.08		
Total	**101.45**	**100.72**	**101.42**	**99.01**	**97.98**	**99.09**	**98.42**	**85.38**	**100.23**	**98.87**	**99.46**	**100.23**	**99.03**	**101.17**	**98.79**	**97.77**	**98.48**	**100.93**	**100.23**	**100.70**	**101.75**	**102.23**	**98.39**	**98.08**
#O	*4*	*6*	*6*	*4*	*23*	*23*	*23*	*7*	*4*	*23*	*23*	*4*	*6*	*4*	*23*	*23*	*23*	*4*	*6*	*6*	*12*	*4*	*23*	*23*
#Si	0.995	1.958	1.982	0.004	6.448	8.038	7.730	1.927	0.003	6.475	7.914	0.995	1.968	0.003	8.001	6.652	7.957	0.995	1.969	1.902	2.981	0.004	6.415	7.893
#Ti	0.000	0.000	0.002	0.002	0.008	0.001	0.006	0.004	0.001	0.008	0.001	0.000	0.000	0.046	0.000	0.007	0.002	0.000	0.000	0.000	0.002	0.003	0.017	0.001
#Al	0.000	0.052	0.032	0.855	2.106	0.000	0.334	0.071	0.930	2.059	0.113	0.000	0.047	0.106	0.020	1.767	0.028	0.000	0.069	0.206	1.953	0.925	2.354	0.196
#Fe^{3+}	0.000	0.000	0.000	0.096	0.000	0.000	0.000	0.000	0.107	0.000	0.000	0.000	0.000	0.825	0.000	0.000	0.000	0.000	0.000	0.000	0.000	0.084	0.000	0.000
#Cr	0.000	0.009	0.018	1.037	0.168	0.008	0.045	0.059	0.953	0.164	0.039	0.000	0.008	0.969	0.000	0.133	0.014	0.000	0.000	0.005	0.028	0.979	0.151	0.011
#Fe^{2+}	0.175	0.169	0.054	0.517	0.394	0.776	0.188	0.302	0.477	0.365	0.176	0.269	0.238	0.892	1.089	0.632	0.312	0.231	0.197	0.101	0.618	0.531	0.422	0.220
#Mn	0.003	0.005	0.002	0.007	0.018	0.026	0.001	0.000	0.009	0.004	0.004	0.004	0.006	0.015	0.053	0.010	0.011	0.003	0.003	0.003	0.023	0.009	0.004	0.006
#Ca	0.000	0.011	0.864	0.004	1.866	0.079	1.934	0.002	0.000	1.906	1.866	0.000	0.009	0.001	0.096	1.870	1.848	0.000	0.011	0.820	0.445	0.000	1.880	1.960
#Mg	1.824	1.804	1.030	0.475	4.056	6.015	4.759	2.635	0.517	4.057	4.875	1.732	1.725	0.138	5.727	3.993	4.790	1.770	1.748	0.945	1.974	0.464	3.838	4.707
#Ni	0.008	0.003	0.002	0.002	0.000	0.012	0.012	0.004	0.002	0.010	0.005	0.006	0.003	0.005	0.000	0.008	0.012	0.006	0.000	0.000	0.000	0.002	0.000	0.000
#Na	0.000	0.000	0.014	0.000	0.666	0.000	0.124	0.000	0.000	0.701	0.030	0.000	0.000	0.000	0.000	0.637	0.093	0.000	0.000	0.020	0.000	0.000	0.455	0.018
#K	0.000	0.000	0.001	0.000	0.023	0.000	0.007	0.000	0.000	0.014	0.000	0.000	0.000	0.000	0.005	0.000	0.000	0.000	0.000	0.000	0.001	0.000	0.013	0.002
Total	3.005	4.011	3.999	3.000	15.752	14.957	15.139	5.004	3.000	15.763	15.024	3.005	4.004	3.000	14.991	15.709	15.067	3.005	3.997	4.003	8.026	3.000	15.549	15.013
Mg# [b]	*0.912*	*0.914*	*0.950*	*0.479*	*0.912*	*0.886*	*0.962*	*0.897*	*0.520*	*0.917*	*0.965*	*0.865*	*0.879*	*0.134*	*0.840*	*0.863*	*0.939*	*0.885*	*0.898*	*0.904*	*0.761*	*0.466*	*0.901*	*0.955*
Cr# [c]		0.145	0.358	0.548	0.074		0.120	0.457	0.506	0.074	0.255		0.139	0.901		0.070	0.332	0.402		0.022	0.014	0.514	0.060	0.052
T°C				660					690					690								720		
ΔNNO				+ 0.4					+ 0.8					+ 3.3								- 0.3		

[a] All Fe as FeO except for spinels for which Fe_2O_3 is calculated from stoichiometry. [b] Mg# = Mg/(Mg+Fe^{2+}). [c] Cr# = Cr/(Cr+Al). [d] T°C and ΔNNO are closure temperature and oxygen fugacity relative to Ni-NiO buffer, respectively, calculated from ol-opx-spinel equilibrium following Ballhaus et al. (1991), and calculated for the average spinel composition of the sample. Mineral abbreviations: ol = olivine, Opx = orthopyroxene, Cpx = clinopyroxene, Cr = Cr-spinel, Hbl = hornblende, Trem = tremolite, Antp = anthophyllite, Grt = garnet

Table 4. Summary of potentially diagnostic features of tectonic settings [a]

Tectonic setting	Oceanic/abyssal	SSZ (including ophiolites)	SBUC, Pohorje
MgO/SiO_2 below terrestrial array	Common (sea-floor weathering)	Possible (metamorphic overprint, weathering)	Harzburgites below terrestrial arry
Melt depletion parameters			
High whole-rock MgO/SiO_2	Values >1.1 rare but common in some localities	Values >1.1 common	All values <1.0
High Cr# spinel	Typical range 20-50	Typical range 30-80	Mostly 35-55
Geochemical parameters			
Li, Pb, U anomalies	Ubiquitous (seawater interaction)	Possibly enriched in slab-derived and crustal fluids	Ubiquitous
Negative Ce anomalies	Ubiquitous (seawater interaction)	Rare (subducted deep-sea sediments)	In two out of five samples
Negative HFSE anomalies	Not uncommon	Common but not ubiquitous	Only for Zr
Fluid-mobile elements	As, Sb, Pb enriched	As, Sb, Pb strongly enriched (from slab-derived fluids)	As, Sb, Pb enriched
Oxidation state	Typically < ΔNNO	ΔNNO = -0.5 to 1.0	No reliable estimate

[a] For detailed discussion and references see main text

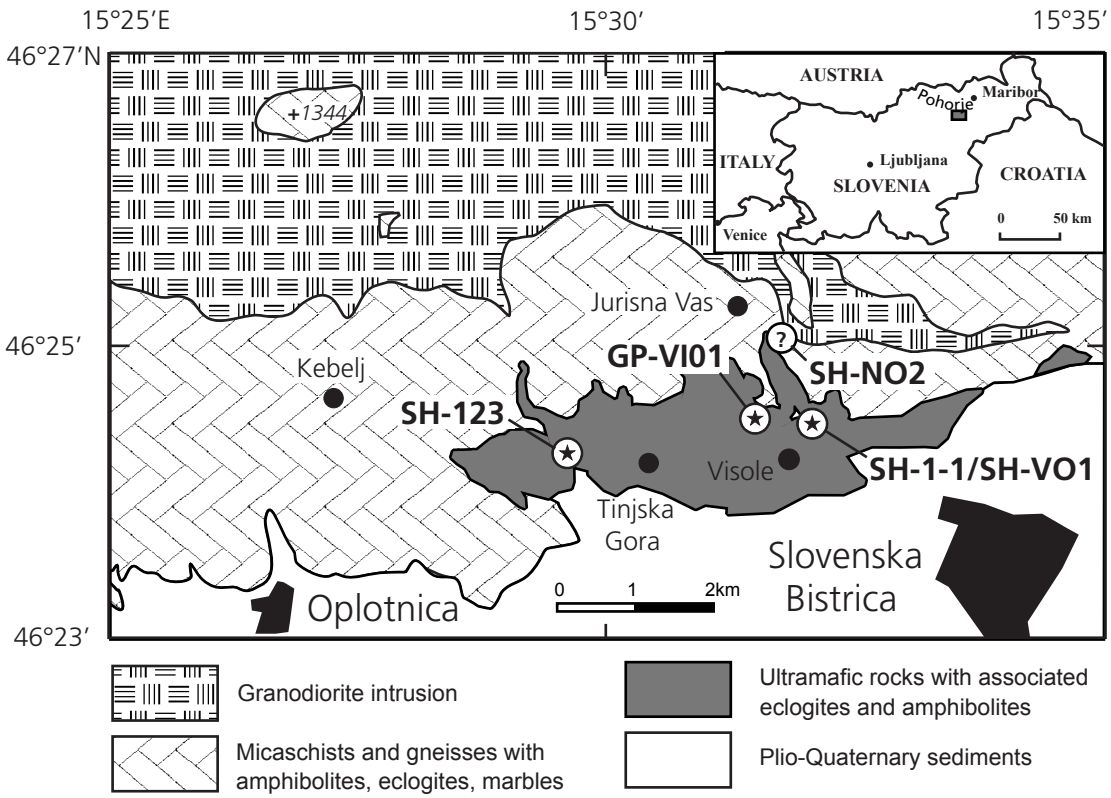

Fig. 1. De Hoog et al. Pohorje serpentinites

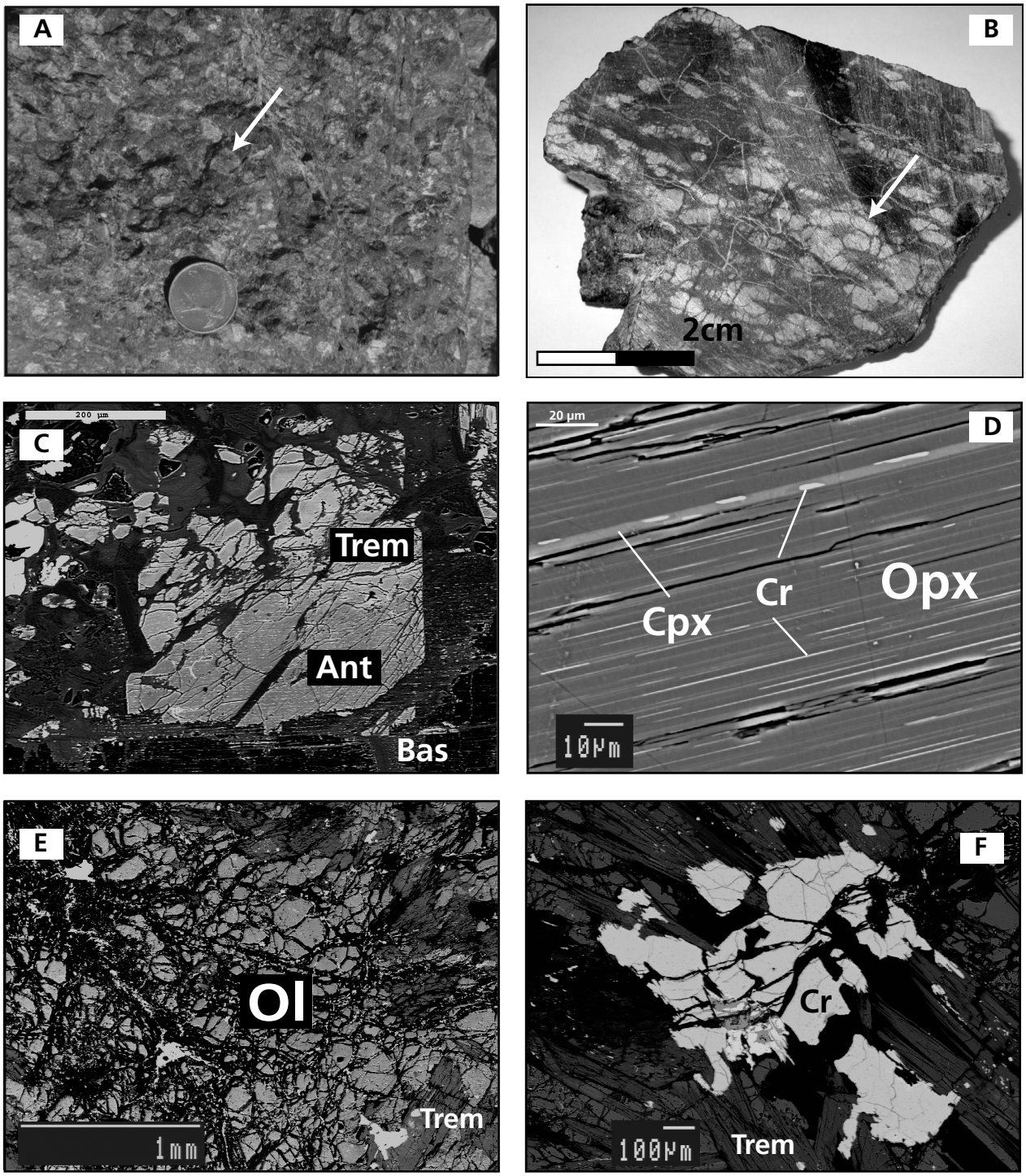

Fig 2. De Hoog et al. Pohorje serpentinites

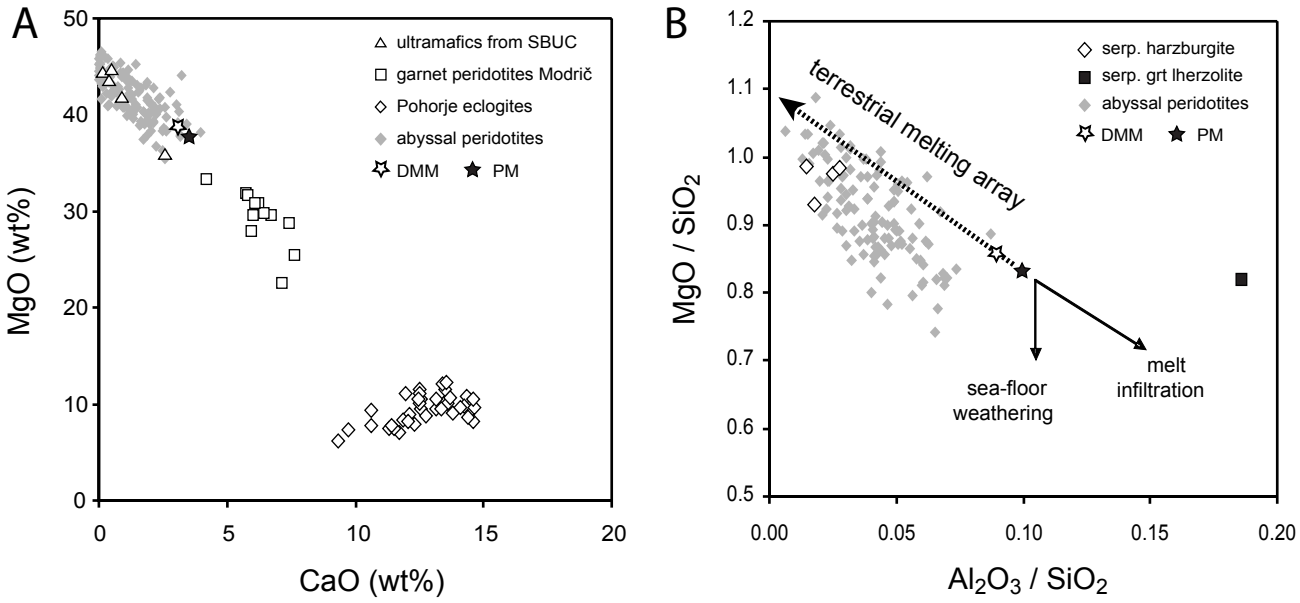

Fig 3. De Hoog et al. Pohorje serpentinites

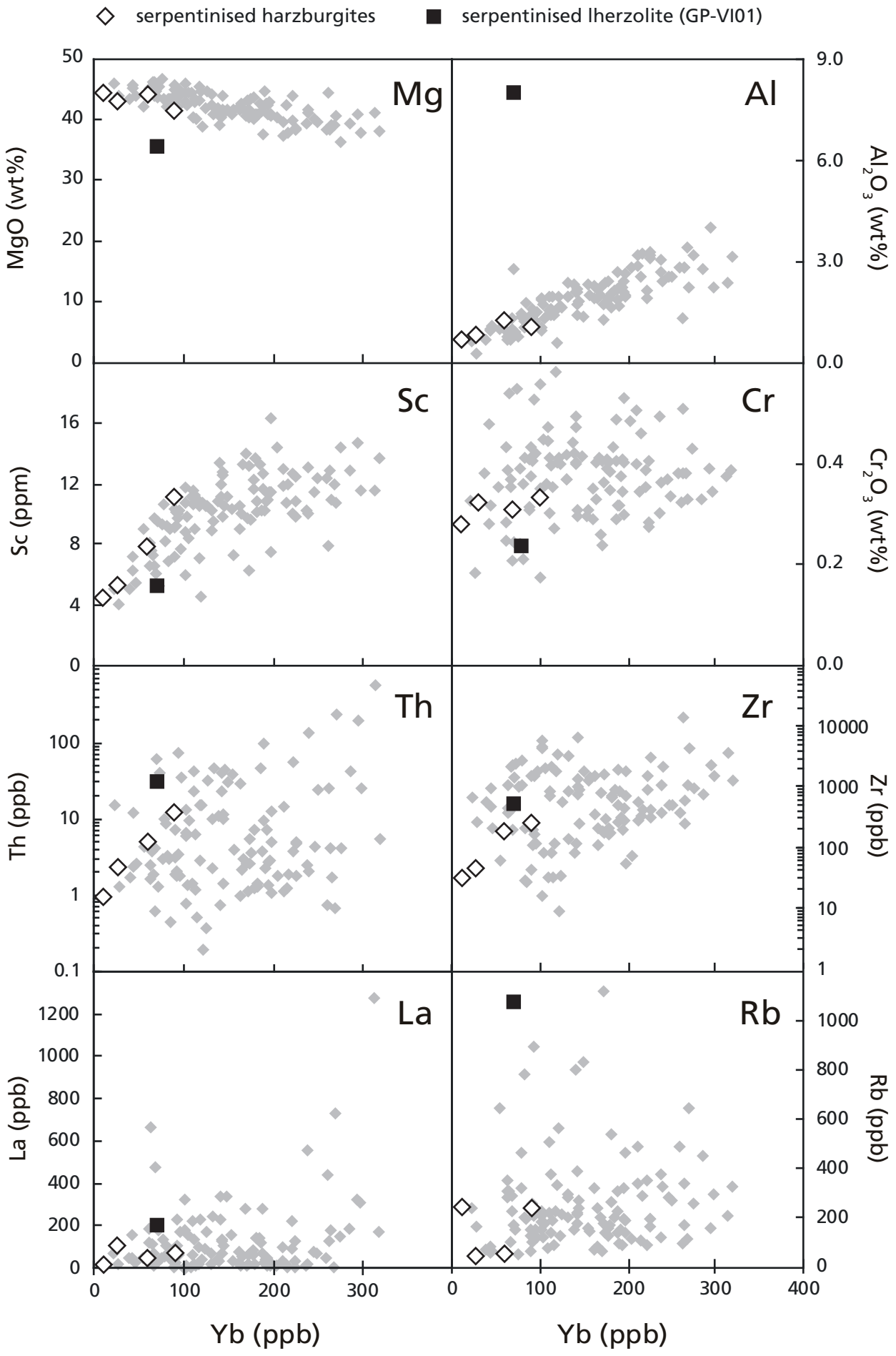

Fig. 4. De Hoog et al. Pohorje serpentinites

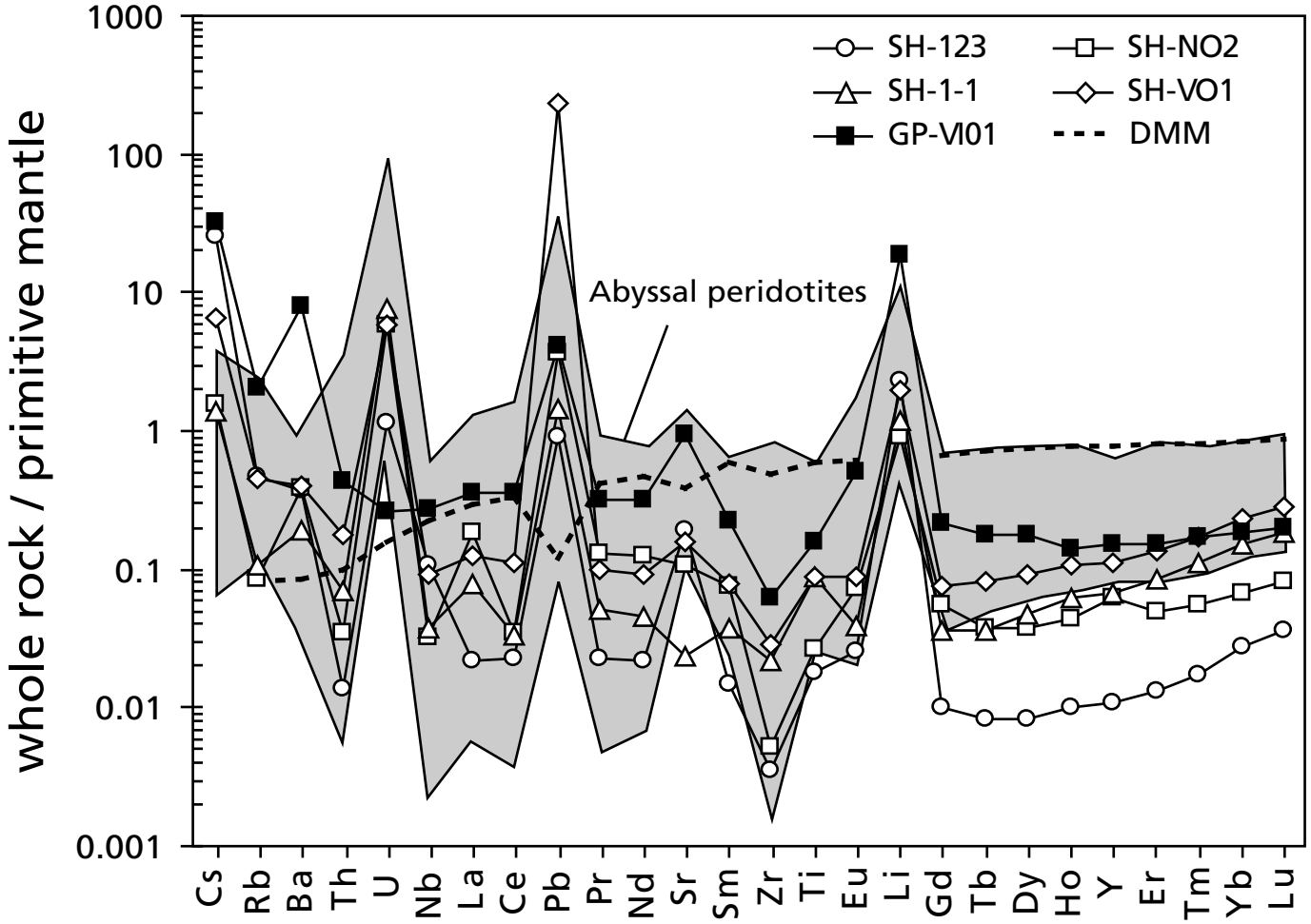

Fig 5. De Hoog et al. Pohorje serpentinites

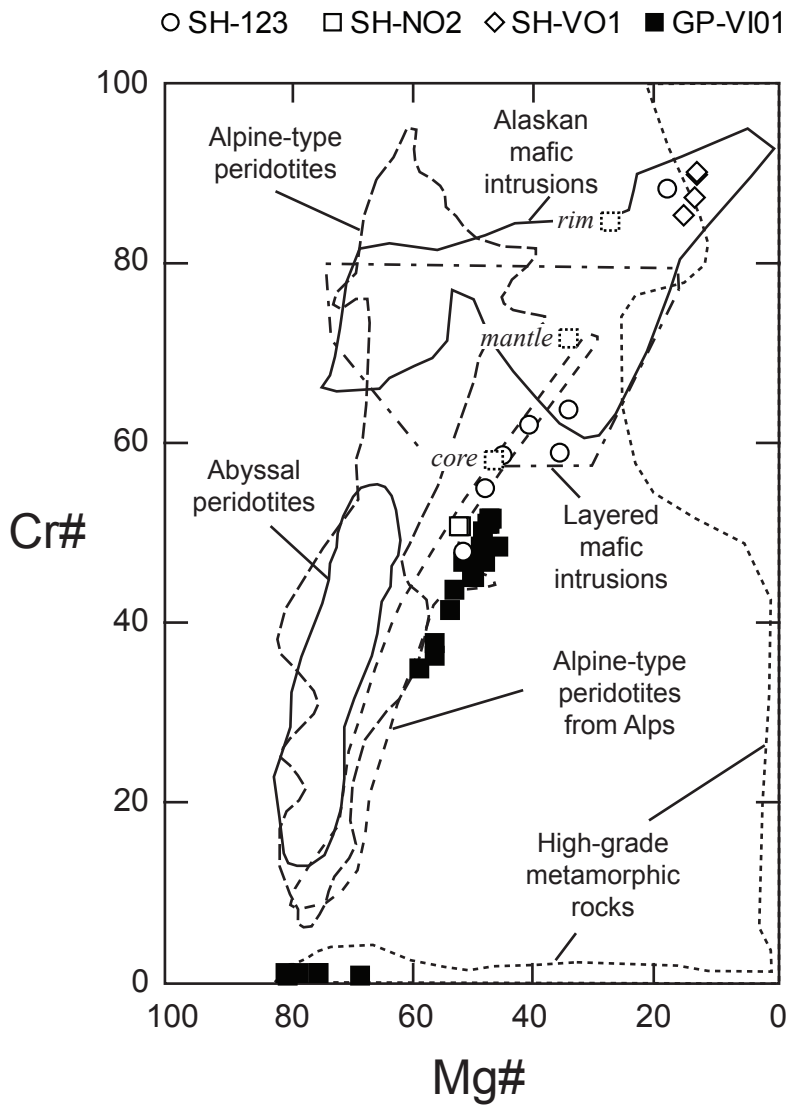

Fig 6. De Hoog et al. Pohorje serpentinites

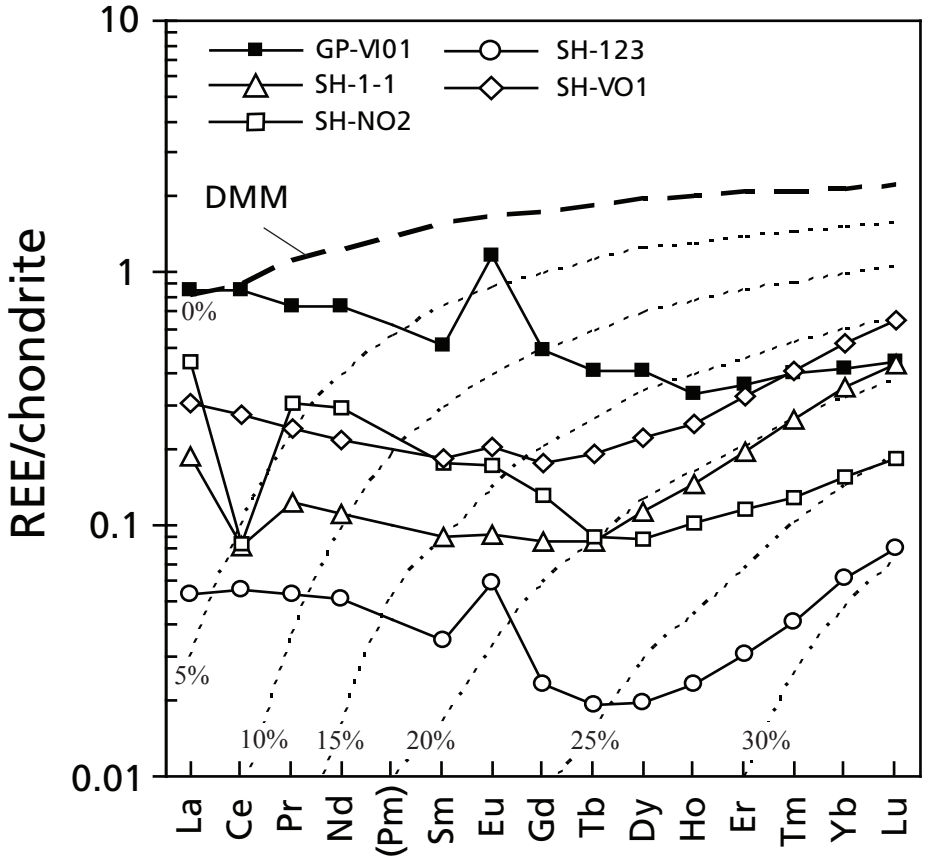

Fig. 7. De Hoog et al. Pohorje serpentinites

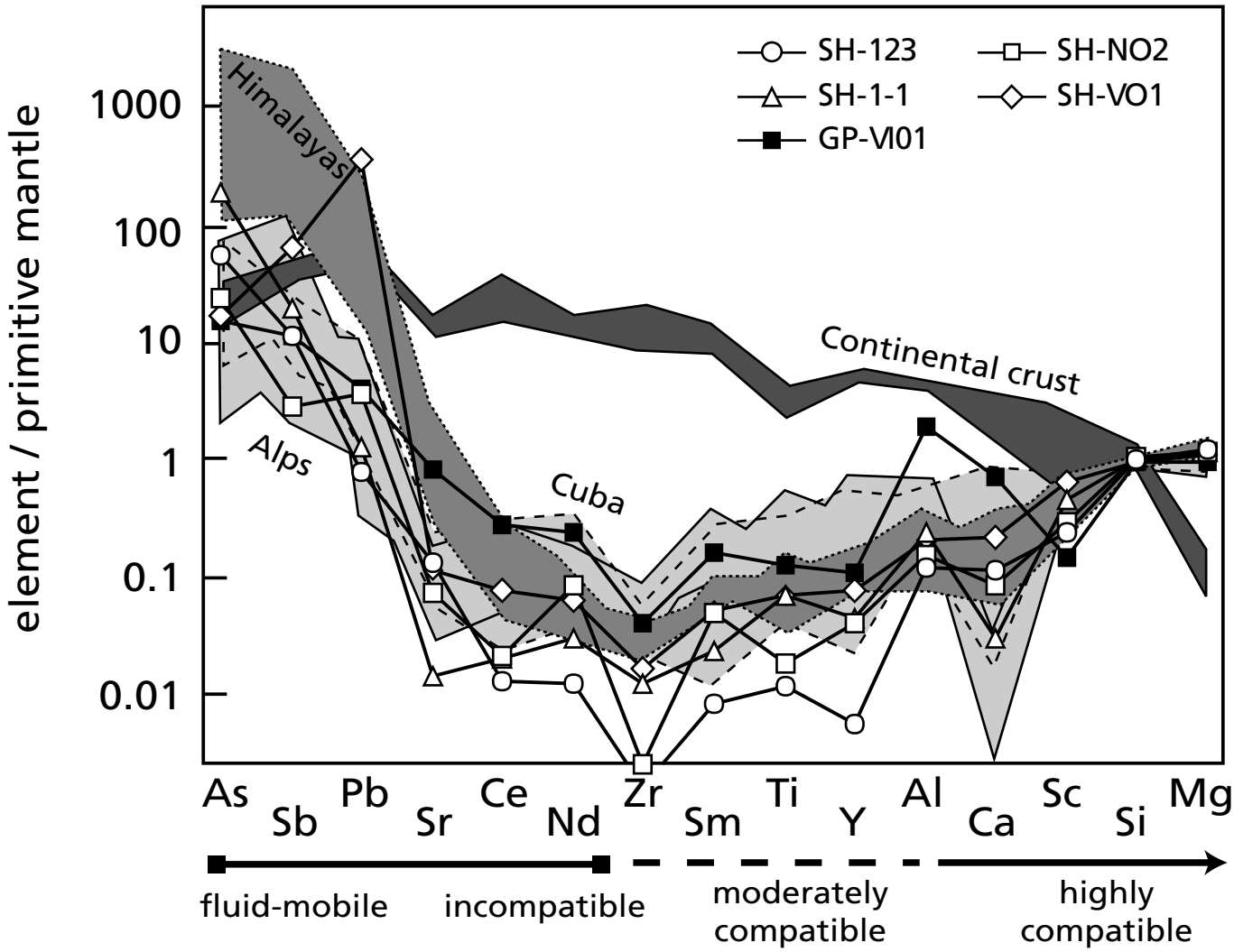

Fig 8. De Hoog et al. Pohorje serpentinites

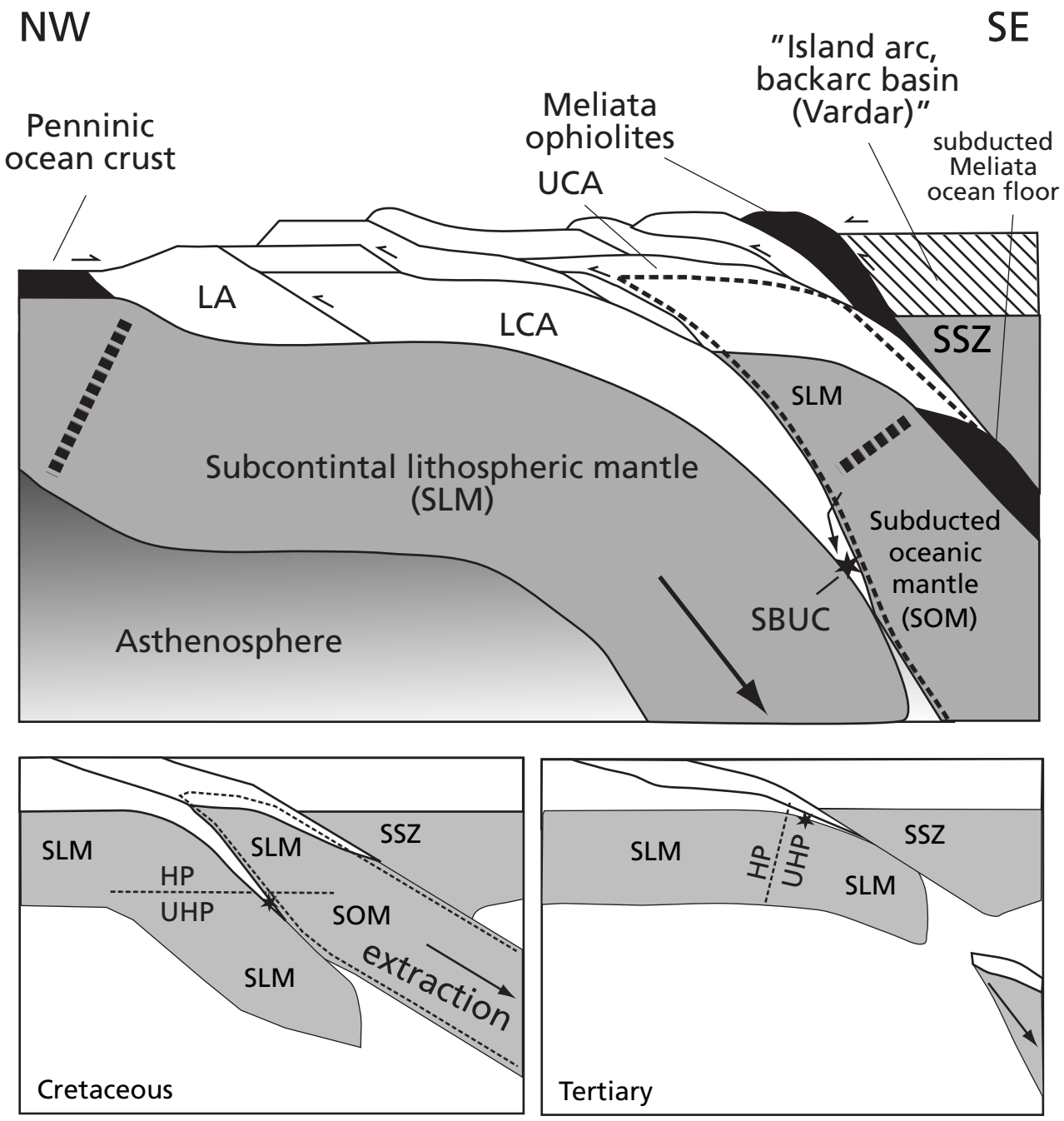

Fig. 9. De Hoog et al. Pohorje serpentinites